

Phosphonated Chelates for Nuclear Imaging

Sabah Abada,^a Alexandre Lecointre,^a Cécile Christine,^{a*} Laurence Ehret-Sabatier,^b Falk Saupe,^c Gertraud Orend,^c David Brasse,^d Ali Ouadi,^d Thomas Hussenet,^c Patrice Laquerrière,^d Mourad Elhabiri^{e*} and Loïc J. Charbonnière^{a*}

Supplementary Information (41 pages including this one)

Figure S1. Potentiometric titration curve and Hyperquad analysis of the cupric complexes formed with ligands **L**¹-**L**⁴. Solvent: H₂O; *I* = 0.1 M (NaClO₄); *T* = 25.0(2) °C; [**L**¹]_{tot} = 2.12 × 10⁻³ M; [**L**²]_{tot} = 2.44 × 10⁻³ M; [**L**³]_{tot} = 2.03 × 10⁻³ M and [**L**⁴]_{tot} = 7.97 × 10⁻⁴ M.

Figure S2. Distribution diagrams as a function of pH of the protonated cupric complexes formed with ligands **L**¹, **L**², **L**³ and **L**⁴. Solvent: H₂O; *T* = 25.0(2) °C; *I* = 0.1 M (NaClO₄). [**L**] = [Cu] = 2 × 10⁻³ M.

Figure S3. Distribution diagrams as a function of pH of the protonated nickel(II) complexes formed with ligands **L**¹, **L**², **L**³ and **L**⁴. Solvent: H₂O; *T* = 25.0(2) °C; *I* = 0.1 M (NaClO₄). [**L**] = [Ni] = 2 × 10⁻³ M.

Figure S4. Distribution diagrams as a function of pH of the protonated zinc(II) complexes formed with ligands **L**¹, **L**², **L**³ and **L**⁴. Solvent: H₂O; *T* = 25.0(2) °C; *I* = 0.1 M (NaClO₄). [**L**] = [Zn] = 2 × 10⁻³ M.

Figure S5. Distribution diagrams as a function of pH of the protonated cobalt(II) complexes formed with ligands **L**¹ and **L**². Solvent: H₂O; *T* = 25.0(2) °C; *I* = 0.1 M (NaClO₄). [**L**] = [Co] = 2 × 10⁻³ M.

Figure S6. Absorption vs. pH titration of the cupric complexes formed with **L**¹ and absorbances at 350 and 750 nm as a function of pH. Solvent: H₂O; *I* = 0.1 M (NaClO₄); *T* = 25.0(2) °C; *l* = 1 cm. [**L**¹]_{tot} = 1.41 × 10⁻⁴ M; [Cu(II)]_{tot} = 1.40 × 10⁻⁴ M; (1) pH = 2.59; (2) pH = 11.17.

Figure S7. Absorption vs. pH titrations of the cupric complexes formed with L^2 and absorbances at 350 and 750 nm as a function of pH. Solvent: H_2O ; $I = 0.1$ M ($NaClO_4$); $T = 25.0(2)$ °C; $l = 1$ cm. $[L^2]_{tot} = 1.39 \times 10^{-4}$ M; $[Cu(II)]_{tot} = 1.30 \times 10^{-4}$ M; (1) pH = 4.15; (2) pH = 9.19.

Figure S8. Absorption vs. pH titrations of the cupric complexes formed with L^3 and absorbances at 350 and 700 nm as a function of pH. Solvent: H_2O ; $I = 0.1$ M ($NaClO_4$); $T = 25.0(2)$ °C; $l = 1$ cm. $[L^3]_{tot} = [Cu(II)]_{tot} = 1.78 \times 10^{-4}$ M; (1) pH = 2.49; (2) pH = 11.19.

Figure S9. Absorption vs. pH titrations of the cupric complexes formed with L^4 and absorbances at 300 and 700 nm as a function of pH. Solvent: H_2O ; $I = 0.1$ M ($NaClO_4$); $T = 25.0(2)$ °C; $l = 1$ cm. $[L^3]_{tot} = [Cu(II)]_{tot} = 1.30 \times 10^{-4}$ M; (1) pH = 2.49; (2) pH = 12.16.

Figure S10. Cyclic voltamperograms of CuL^1 , CuL^2 , CuL^3 and CuL^4 measured in water at pH ~ 3.7. Solvent: H_2O ; $I = 0.1$ M ($NaClO_4$); $T = 25.0(2)$ °C; reference = Ag/AgCl; $[CuL^1]_{tot} = 9.94 \times 10^{-4}$ M; $v = 200$ mV.

Figure S11. CV of CuL^1 as a function of pH. Solvent: H_2O ; $I = 0.1$ M ($NaClO_4$); $T = 25.0(2)$ °C; reference = Ag/AgCl; $[CuL^1]_{tot} = 9.94 \times 10^{-4}$ M; $v = 200$ mV.

Figure S12. (a) Variation of the pM values ($M = Cu^{II}$, Zn^{II} , Ni^{II} , Co^{II} and Ga^{III}) as a function of pH for ligand L^2 . Solvent: H_2O ; $I = 0.1$ M; $T = 25.0(2)$ °C; $pM = -\log[M^{II}]_{free}$ or $-\log[M^{III}]_{free}$, $[L]_{tot} = 10^{-5}$ M and $[M^{II}]_{tot}$ or $[M^{III}]_{tot} = 10^{-6}$ M.

Figure S13. (a) Variation of the pM values ($M = Cu^{II}$, Zn^{II} , Ni^{II}) as a function of pH for ligand L^3 . Solvent: H_2O ; $I = 0.1$ M; $T = 25.0(2)$ °C; $pM = -\log[M^{II}]_{free}$ or $-\log[M^{III}]_{free}$, $[L]_{tot} = 10^{-5}$ M and $[M^{II}]_{tot}$ or $[M^{III}]_{tot} = 10^{-6}$ M.

Figure S14. (a) Variation of the pM values ($M = Cu^{II}$, Zn^{II} , Ni^{II}) as a function of pH for ligand L^4 . Solvent: H_2O ; $I = 0.1$ M; $T = 25.0(2)$ °C; $pM = -\log[M^{II}]_{free}$ or $-\log[M^{III}]_{free}$, $[L]_{tot} = 10^{-5}$ M and $[M^{II}]_{tot}$ or $[M^{III}]_{tot} = 10^{-6}$ M.

Figure S15 to 44. 1H , ^{13}C and ^{31}P NMR spectra of the compounds.

Table S1. Intensity maxima of the ESI-MS pseudo-molecular ions of the metallic complexes formed with ligands L^1 - L^4 .

Table S2. Stability and protonation constants of the metallic complexes with Ni(II), Zn(II), Co(II) formed with ligands L^1 - L^4 .

Physico-chemicals Investigations

Starting Materials and Solvents. Copper(II) perchlorate ($\text{Cu}(\text{ClO}_4)_2 \cdot 6\text{H}_2\text{O}$, FLUKA, purum p.a.), zinc(II) perchlorate ($\text{Zn}(\text{ClO}_4)_2 \cdot 6\text{H}_2\text{O}$, VENTRON, ALFA PRODUKTE, 98.9%), cobalt(II) ($\text{Co}(\text{ClO}_4)_2 \cdot 6\text{H}_2\text{O}$, Fluka, purum p.a.) and nickel(II) perchlorate ($\text{Ni}(\text{ClO}_4)_2 \cdot 6\text{H}_2\text{O}$, FLUKA, purum p.a.) are commercial products, which were used without further purification. Distilled water was further purified by passing it through a mixed bed of ion-exchanger (BIOBLOCK Scientific R3-83002, M3-83006) and activated carbon (BIOBLOCK Scientific ORC-83005) and was de-oxygenated by CO_2 - and O_2 -free argon (SIGMA Oxiclear cartridge) before use. All the stock solutions were prepared by weighing solid products using an AG 245 METTLER TOLEDO analytical balance (precision 0.01 mg). The ionic strength was maintained at 0.1 M with sodium perchlorate ($\text{NaClO}_4 \cdot \text{H}_2\text{O}$, MERCK, p.a.), and all measurements were carried out at 25.0(2) °C. The metal stock solutions ($\sim 3\text{-}6 \times 10^{-2}$ M) were freshly prepared by dissolution of appropriate amounts of the corresponding solid perchlorate or nitrate salts in water saturated with argon. The metal contents of the solutions were determined according to the classical colorimetric titrations.¹

*CAUTION! Perchlorate salts combined with organic ligands are potentially explosive and should be handled in small quantities and with the adequate precautions.*²

Potentiometric Titrations. The potentiometric titrations of ligands L^1 ($2.2\text{-}2.5 \times 10^{-3}$ M), L^2 ($2.3\text{-}2.5 \times 10^{-3}$ M), L^3 ($1.6\text{-}2.5 \times 10^{-3}$ M), L^4 ($0.97\text{-}1.69 \times 10^{-3}$ M) and their metal complexes ($1.4 < [\text{L}]_{\text{tot}}/[\text{M}]_{\text{tot}} < 0.8$) were performed using an automatic titrator system 794 Basic Titrino (METROHM) with a combined glass electrode (METROHM 6.0234.500, Long Life) filled with 0.1 M NaCl in water and connected to a microcomputer (TIAMO light 1.2 program for the acquisition of the potentiometric data). The combined glass electrode was calibrated as a hydrogen concentration probe by titrating known amounts of perchloric acid ($\sim 1.3 \times 10^{-2}$ M from HClO_4 , PROLABO, normapur, 70% min) with CO_2 -free sodium hydroxide solution ($\sim 10^{-1}$ M from NaOH, BDH, AnalaR).³ The HClO_4 and NaOH solutions were freshly prepared just before use and titrated with sodium tetraborate decahydrate ($\text{B}_4\text{Na}_2\text{O}_7 \cdot 10\text{H}_2\text{O}$, FLUKA, puriss, p.a.) and potassium hydrogen phthalate ($\text{C}_8\text{H}_5\text{KO}_3$, FLUKA, puriss, p.a.), respectively, using methyl orange (RAL) and phenolphthalein (PROLABO, purum) as the indicators. The cell was

1 Méthodes d'Analyses Complexométriques avec les Titriplex®, Ed. Merck, Darmstadt.

2 K. N. Raymond, *Chem. Eng. News*, 1983, **61**, 4.

3 P. Gans and B. O'Sullivan, *Talanta*, 2000, **51**, 33.

thermostated at 25.0 ± 0.2 °C by the flow of a LAUDA E200 thermostat. A stream of argon, pre-saturated with water vapor, was passed over the surface of the solution. The GLEE program³ was applied for the glass electrode calibration (standard electrode potential E_0/mV and slope of the electrode/ mV pH^{-1}) and to check carbonate levels of the NaOH solutions used ($< 5\%$). The potentiometric data of $\mathbf{L}^1\text{-L}^4$ and their metal complexes (about 300 points collected over the pH range 2.5-11.5) were refined with the HYPERQUAD 2000⁴ program which uses non-linear least-squares methods.⁵ Potentiometric data points were weighted by a formula allowing greater pH errors in the region of an end-point than elsewhere. The weighting factor W_i is defined as the reciprocal of the estimated variance of measurements: $W_i = 1/\sigma_i^2 = 1/[\sigma_E^2 + (\delta E/\delta V)^2\sigma_V^2]$ where σ_E^2 and σ_V^2 are the estimated variances of the potential and volume readings, respectively. The constants were refined by minimizing the error-square sum, U , of the potentials: $U = \sum_i^N W_i (E_{\text{obs},i} - E_{\text{cal},i})^2$. At least two to three titrations were treated as single sets or as separated entities, for each system, without significant variation in the values of the determined constants. The quality of fit was judged by the values of the sample standard deviation, S , and the goodness of fit, χ^2 , (Pearson's test). At $\sigma_E = 0.1$ mV ($0.023 \sigma_{\text{pH}}$) and $\sigma_V = 0.005$ mL, the values of S in different sets of titrations were between 0.8 and 1.2, and χ^2 was below 20. The scatter of residuals versus pH was reasonably random, without any significant systematic trends, thus indicating a good fit of the experimental data. The successive protonation constants were calculated from the cumulative constants determined with the program. The uncertainties in the log K values correspond to the added standard deviations in the cumulative constants. The distribution curves of the protonated species of $\mathbf{L}^1\text{-L}^4$ and their metal complexes as a function of pH were calculated using the Hyss program.⁶

Spectrophotometric Titrations versus pH. Spectrophotometric titrations as a function of pH of the free ligands $\mathbf{L}^1\text{-L}^4$ were first performed. Stock solutions of \mathbf{L}^1 (1.51×10^{-4} M), \mathbf{L}^2 (1.34×10^{-4} M), \mathbf{L}^3 (2.29×10^{-4} M) or \mathbf{L}^4 (1.76×10^{-4} M) were prepared by quantitative dissolution of the corresponding solid samples in deionised water and the ionic strength was adjusted to

-
- 4 (a) P. Gans, A. Sabatini and A. Vacca, *HYPERQUAD2000*. Leeds, U.K., and Florence, Italy, 2000. (b) P. Gans, A. Sabatini and A. Vacca, *Talanta*, 1996, **43**, 1739.
5 P. Gans, *Data Fitting in the Chemical Sciences*, John Wiley & Sons, Chichester, 1992.
6 L. Alderighi, P. Gans, A. Ienco, D. Peters, A. Sabatini and A. Vacca, *Coord. Chem. Rev.* 1999, **184**, 311.

0.1 M with NaClO₄ (Fluka, puriss). 40 mL of the solutions were introduced into a jacketed cell (METROHM) maintained at 25.0 ± 0.2 °C (LAUDA E200). The free hydrogen ion concentration was measured with a combined glass electrode (METROHM 6.0234.500, Long Life) and an automatic titrator system 794 Basic Titrino (METROHM). The Ag/AgCl reference glass electrode was filled with NaCl (0.1 M, FLUKA, p.a.) and was calibrated as a hydrogen concentration probe as described above. The initial pH was adjusted to ~ 2 with HClO₄ (PROLABO, normapur, 70% min), and the titrations of the free ligands (2.5 < pH < 11.8) were then carried out by addition of known volumes of NaOH solutions (BDH, AnalaR) with an EPPENDORF microburette. Special care was taken to ensure that complete equilibration was attained. Absorption spectra versus pH were recorded using a Varian CARY 50 spectrophotometer fitted with Hellma optical fibers (Hellma, 041.002-UV) and an immersion probe made of quartz suprazil (Hellma, 661.500-QX). The temperature was maintained at 25.0(2) °C with the help of a LAUDA E200 thermostat.

Spectrophotometric titrations of the cupric complexes with ligands **L**¹-**L**⁴ were thereafter carried out. About 40 mL of solutions containing one equivalent of Cu(II) perchlorate and the ligand **L**ⁱ (i = 1-4) (for **L**¹: [**L**¹]₀ = 1.41 × 10⁻⁴ M, [Cu(II)]_{tot} = 1.40 × 10⁻⁴ M, 2.59 < pH < 11.17); for **L**²: [**L**²]₀ = 1.39 × 10⁻⁴ M, [Cu(II)]₀ = 1.30 × 10⁻⁴ M, 4.0 < pH < 9.5; for **L**³: [**L**³]₀ = [Cu(II)]₀ = 1.78 × 10⁻⁴ M, 2.49 < pH < 11.19; for **L**⁴: [**L**⁴]₀ = [Cu(II)]₀ = 1.3 × 10⁻⁴ M, 2.67 < pH < 9.72) were introduced in a jacketed cell (METROHM) maintained at 25.0(2) °C (LAUDA E200). The free hydrogen ion concentration was measured with a combined glass electrode (METROHM 6.0234.500, Long Life) and an automatic titrator system 794 Basic Titrino (METROHM). The initial pH was adjusted to ~ 2-3 with HClO₄ (PROLABO, normapur, 70% min), and the titrations of the cupric complexes were then carried out by addition of known volumes of NaOH solutions (BDH, AnalaR) with an EPPENDORF microburette. Special care was taken to ensure that complete equilibration was attained. Absorption spectra versus pH were recorded using a Varian CARY 50 spectrophotometer.

Analysis and Processing of the Spectroscopic Data. The spectrophotometric data were analyzed with SPECFIT^{7,8,9} program which adjusts the absorptivities and the stability constants of the species formed at equilibrium. SPECFIT uses factor analysis to reduce the absorbance

7 H. Gampp, M. Maeder, C. J. Meyer and A. D. Zuberbühler, *Talanta*, 1985, **32**, 95.

8 H. Gampp, M. Maeder, C. J. Meyer and A. D. Zuberbühler, *Talanta*, 1985, **32**, 251.

9 H. Gampp, M. Maeder, C. J. Meyer and A. D. Zuberbühler, *Talanta*, 1985, **32**, 1133.

matrix and to extract the eigenvalues prior to the multiwavelength fit of the reduced data set according to the Marquardt algorithm.^{10,11}

Electrospray Mass Spectrometric Measurements. Electrospray mass spectra of metal complexes with L^1-L^4 were obtained with an AGILENT TECHNOLOGIES 6120 quadrupole equipped with an electrospray (ESI) interface. Solutions ($1.8-5 \times 10^{-4}$ M) of the metal complexes (M= Cu(II), Ni(II) and Zn(II)) with L^1-L^4 have been prepared in water in the absence of any background salt. The sample solutions were continuously introduced into the spectrometer source with a syringe pump (KD SCIENTIFIC) with a flow rate of $300 \mu\text{L}\cdot\text{h}^{-1}$. For electrospray ionization, the drying gas was heated at 250°C and its flow was set at $6 \text{ L}\cdot\text{min}^{-1}$. The capillary exit voltage was fixed at 5 kV and the skimmer voltage was varied from 140 to 170 V in order to optimize the signal responses. Scanning was performed from $m/z = 100$ to 1000 and no fragmentation processes were observed under our experimental conditions.

Electrochemistry. Cyclic voltammetry of the cupric complexes with ligands L^1-L^4 ($[\text{Cu}L^1]_0 = 9.94 \times 10^{-4}$ M, $[\text{Cu}L^2]_0 = 1.091 \times 10^{-3}$ M, $[\text{Cu}L^3]_0 = 1.096 \times 10^{-3}$ M, $[\text{Cu}L^4]_0 = 1.063 \times 10^{-3}$ M) were performed using a VOLTALAB 50 potentiostat/galvanostat (RADIOMETER ANALYTICAL MDE15 polarographic stand, PST050 analytical voltammetry and CTV101 speed control unit) controlled by the VOLTAMASTER 4 electrochemical software. A conventional three-electrode cell (10 mL) was employed in our experiments with a glassy carbon disk (GC, $s = 0.071 \text{ cm}^2$) set into a Teflon rotating tube as a working electrode, a Pt wire as a counter electrode, and $\text{KCl}_{(\text{sat})}/\text{Ag}/\text{AgCl}$ reference electrode ($+210 \text{ mV vs NHE}$).¹² Prior to each measurement, the surface of the GC electrode was carefully polished with $0.3 \mu\text{m}$ aluminium oxide suspension (ESCIL) on a silicon carbide abrasive sheet of grit 800/2400. Thereafter, the GC electrode was copiously washed with water and dried with paper towel and argon. The electrode was installed into the voltammetry cell along with a platinum wire counter electrode and the reference. 10 mL of the aqueous solutions containing *ca.* 10^{-3} M of the cupric complexes with L^1-L^4 were vigorously stirred and purged with O_2 -free (Sigma Oxiclear cartridge) argon for 15 minutes before the voltammetry experiment was initiated, and maintained under an argon atmosphere during the measurement procedure. The

10 D. W. Marquardt, *J. Soc. Indust. Appl. Math.*, 1963, **11**, 431.

11 M. Maeder and A. D. Zuberbühler, *Anal. Chem.*, 1990, **62**, 2220.

12 D. T. Sawyer, A. Sobkowiak and J. L. Jr Roberts, *Electrochemistry for Chemists*, 2nd Ed., Wiley, New York, 1995, 192.

voltammograms (cyclic voltammograms - CV - and square wave voltammograms - SWV) were recorded at room temperature (23(1) °C) in water with 100 mM sodium perchlorate (NaClO₄·H₂O, MERCK, p.a.) as supporting and inert electrolyte. For the CV measurements, the voltage sweep rate was varied from 50 to 300 mV.s⁻¹ and several cyclic voltammograms were recorded from +1.0 V to -1.7 V. Peak potentials were measured at a scan rate of 200 mV.s⁻¹ unless otherwise indicated.

Formation and Dissociation kinetics. The formation kinetics of the copper(II) complexes with **L**¹-**L**⁴ were measured on a SX-18MV stopped-flow spectrophotometer from Applied Photophysics. The temperature was maintained at 25.0(2) °C with the help of a Haake thermostat. The formation kinetics of the copper(II) complexes was studied at [H⁺]_{tot} = 9.14 × 10⁻³ M (pH ~ 2.04) and was monitored at λ = 312 nm (**L**¹), 310 nm (**L**²), 303 nm (**L**³) et 312 nm (**L**⁴) for which neither the ligands nor Cu(II) absorb. These λ correspond to the absorption maximum of the **L**→Cu(II) CT band and thereby to the maximum of absorbance difference between the reactants (**L** and Cu(II)) and the products. [Cu**L**¹H₄]²⁻, [Cu**L**²H₂]⁰, [Cu**L**³H₃]⁻, [Cu**L**⁴H₂]²⁻ are the major species at pH 2.0, while Cu²⁺ is the predominant free copper(II) species under our experimental conditions ($K_{\text{Cu}(\text{OH})^+} = 10^{-6.29}$ and $K_{\text{Cu}(\text{OH})_2} = 10^{-13.1}$).¹³ The ligands concentrations were fixed at [**L**¹]₀ = 3.04 × 10⁻⁴ M, [**L**²]₀ = 3.6 × 10⁻⁴ M, [**L**³]₀ = 4.12 × 10⁻⁴ M and [**L**⁴]₀ = 3.27 × 10⁻⁴ M). At least ten times more concentrated solutions of Cu²⁺ with respect to **L**¹-**L**⁴ were used to impose pseudo-first order conditions and the Cu²⁺ concentrations were varied from 3.83 × 10⁻³ to 3.83 × 10⁻² M for **L**¹, from 1.80 × 10⁻³ M to 2.52 × 10⁻² M for **L**², from 2.06 × 10⁻³ M to 1.44 × 10⁻² M for **L**³ and from 1.64 × 10⁻³ M to 8.15 × 10⁻³ M for **L**⁴.

The dissociation reaction of the copper complexes freshly prepared at pH ~ 10 ([Cu**L**¹]₀ = 7.0 × 10⁻⁵ M, [Cu**L**²]₀ = 5.67 × 10⁻⁵ M, [Cu**L**³]₀ = 6.84 × 10⁻⁵ M and [Cu**L**⁴]₀ = 2.04 × 10⁻⁴ M; I = 0.1 M (NaClO₄)) have been carried out by attack of the proton under acidic conditions with perchloric acid. At pH ~ 10, the fully deprotonated complexes ([Cu**L**¹]⁶⁻, [Cu**L**²]²⁻ et [Cu**L**³]⁴⁻) predominate. The dissociation kinetics was monitored on a SX-18MV stopped-flow spectrophotometer (Applied Photophysics) maintained at 25.0(2) °C (Lauda M12 thermostat) and with a 1 cm optical cell. Pseudo-first order conditions with respect to the complexes were

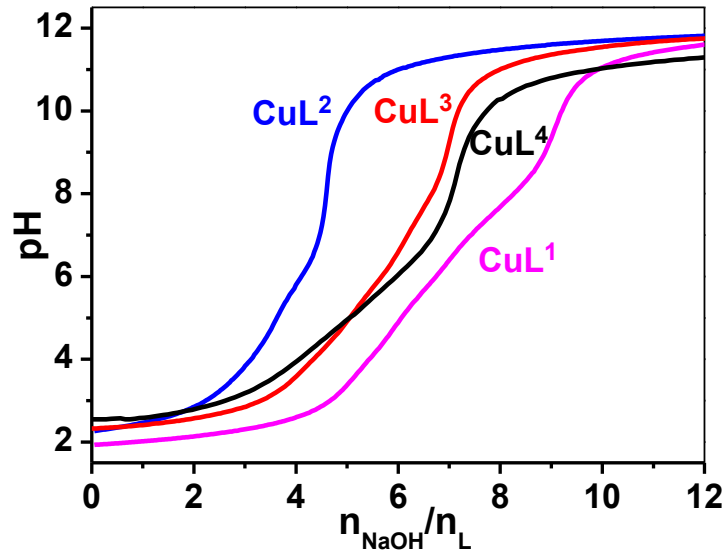
used and HClO_4 concentration was varied from 2×10^{-3} M to 9.6×10^{-1} M. The absorbance decay versus time was monitored at the maximum of the LMCT transitions for each of the cupric complexes.

Analysis and Processing of the kinetic Data. The data sets, averaged out of at least three replicates, were recorded and analyzed with the commercial software Biokine.¹⁴ This program fits up to three exponential functions to the experimental curves with the Simplex algorithm¹⁵ after initialization with a Padé-Laplace method.¹⁶

14 Bio-Logic Company. *Biokine V3.0 User's Manuel*, Ed., Bio-Logic Company, Echirolles, France, 1991.

15 J. A. Nelder and R. Mead, *Comput. J.*, 1965, **7**, 308.

16 E. Yeramian and P. Claverie, *Nature*, 1987, **326**, 169.



CuL^1

Hyperquad2000 - project file e:\sabah1\phoscu2\phoscutot.con

File Project Import Model Potentiometry Run Window Help

Data from e:\sabah1\phoscu2\phoscutot.par

Name new project

Temperature/C 25.0

Maximum number of iterations 25

Excessive beta limit 0.7

Weighting scheme
 automatic
 diagonal
 relative

Betas

Formula	Log Beta	phos	Cu	H	
phos H	11.21	1	0	1	constant
phos H ₂	21.5	1	0	2	constant
phos H ₃	29.54	1	0	3	constant
phos H ₄	36.03	1	0	4	constant
phos H ₅	41.56	1	0	5	constant
phos H ₆	45.75	1	0	6	constant
phos Cu	22.7098	1	1	0	refine
phos Cu H	30.9495	1	1	1	refine
phos Cu H ₂	38.1066	1	1	2	refine
phos Cu H ₃	43.8221	1	1	3	refine
phos Cu H ₄	47.79	1	1	4	constant
Cu H ₋₁	-6.29	0	1	-1	constant
Cu H ₋₂	-13.1	0	1	-2	constant

Manual fitting of potentiometric data

1 Title 3 Plot to clipboard Log beta species
 2 Replot 4 Data to clipboard 43.8221 phos Cu H₃

Speciation and pH data from e:\sabah1\phoscu2\phoscutot.ppd

% formation relative to phos

residuals in pH at selected data points

point number

curve no. 1 - IU/VKV
 point 1. Titre. 005

	% conc.
<input checked="" type="checkbox"/> free phos	0.000
<input checked="" type="checkbox"/> free Cu	
<input checked="" type="checkbox"/> free H	
H ₋₁	
phos H	0.000
phos H ₂	0.000
phos H ₃	0.000
phos H ₄	0.000
phos H ₅	0.034
phos H ₆	5.473
phos Cu	0.000
phos Cu H	0.000
phos Cu H ₂	0.000
phos Cu H ₃	0.961
phos Cu H ₄	93.532
Cu H ₋₁	
Cu H ₋₂	

Curve Label IU/VKV

Initial volume/ml 4.14

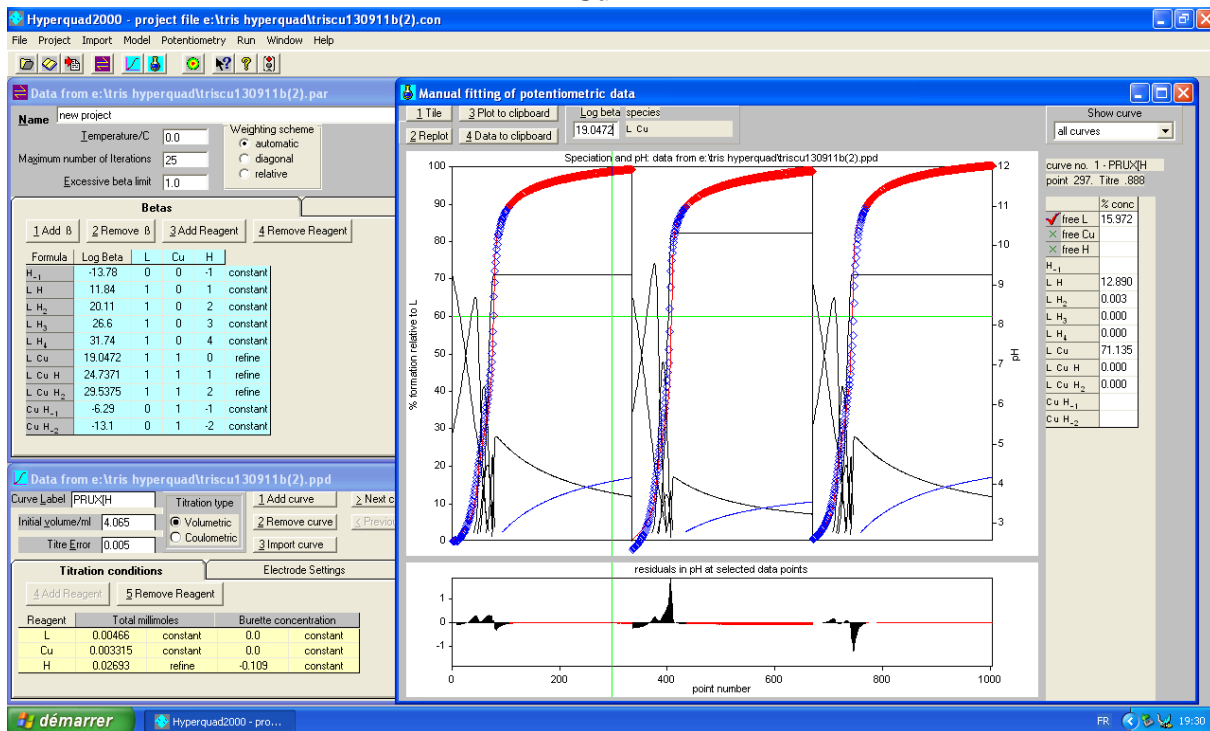
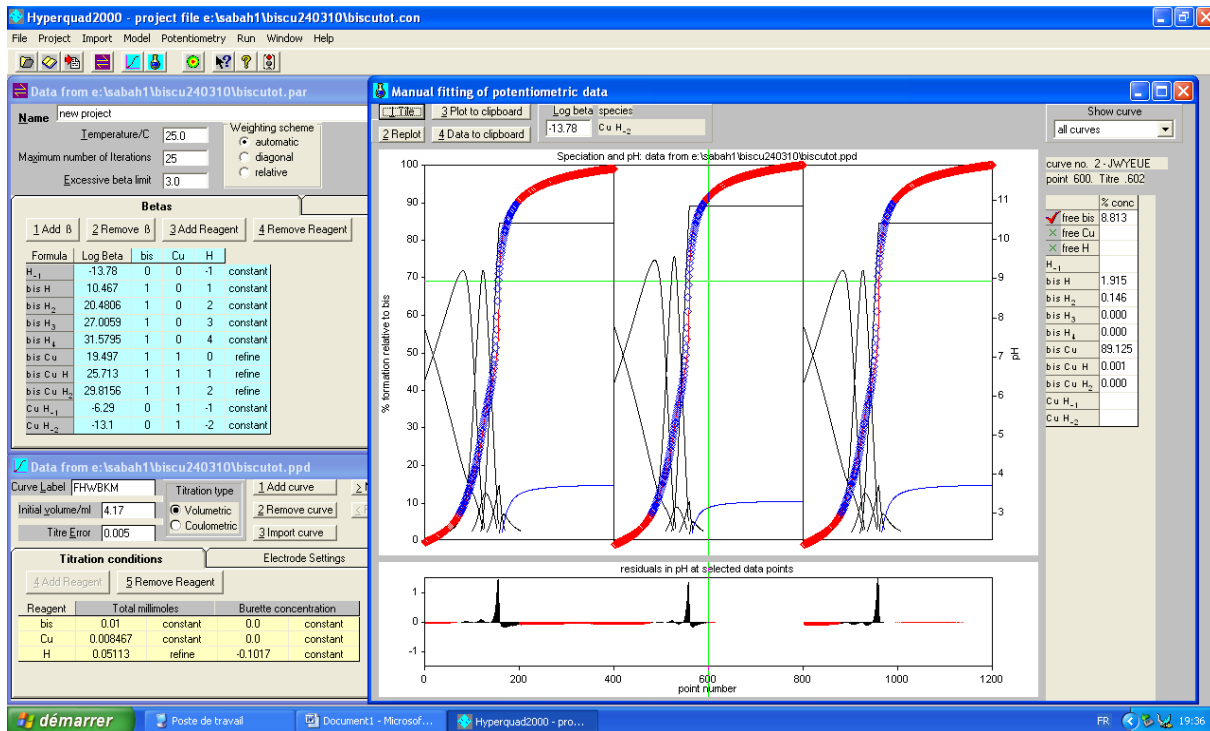
Titration type
 Volumetric
 Coulometric

Titre Error 0.005

Titration conditions

Reagent	Total millimoles	Burette concentration
phos	0.00877	constant 0.0
Cu	0.008358	constant 0.0
H	0.07986	refine -0.0905

démarrer Poste de travail fits.doc - Microsoft W... Hyperquad2000 - pro... FR 19:53



CuL⁴

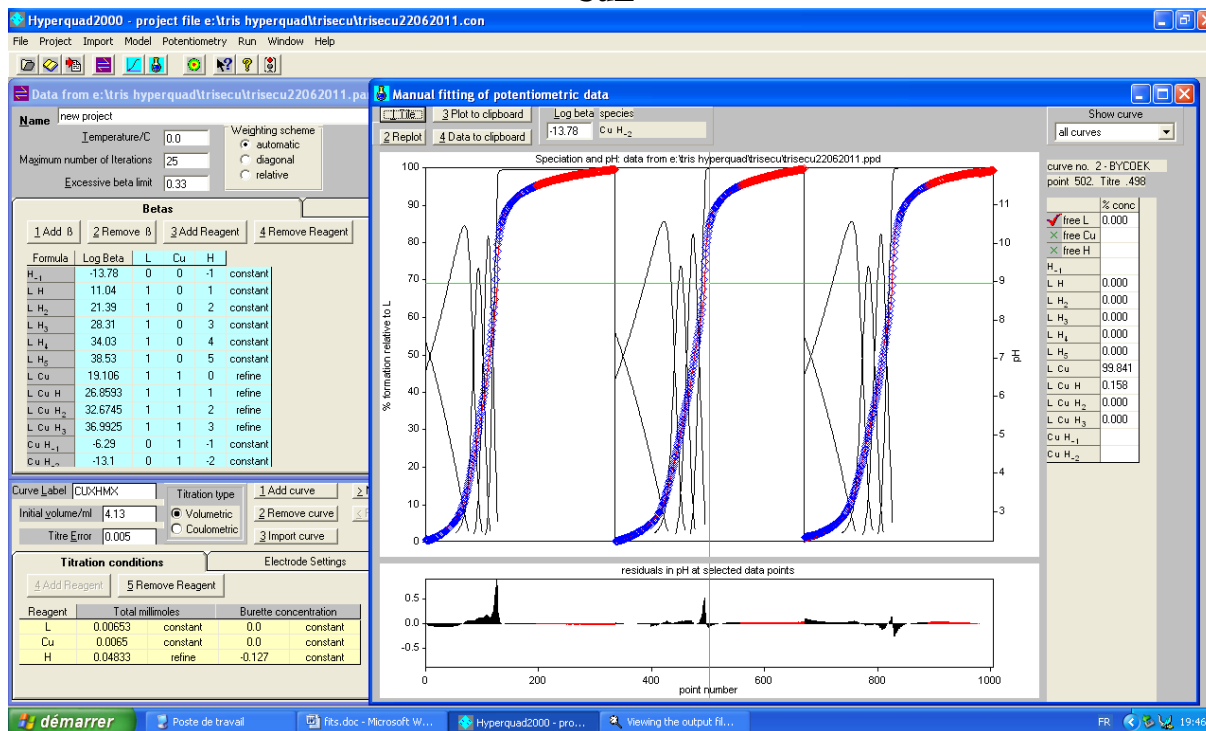


Figure S1. Potentiometric titration curve and Hyperquad analysis of the cupric complexes formed with ligands L^1 - L^4 . Solvent: H_2O ; $I = 0.1$ M ($NaClO_4$); $T = 25.0(2)$ °C; $[L^1]_{tot} = 2.12 \times 10^{-3}$ M ; $[L^2]_{tot} = 2.44 \times 10^{-3}$ M ; $[L^3]_{tot} = 2.03 \times 10^{-3}$ M and $[L^4]_{tot} = 7.97 \times 10^{-4}$ M.

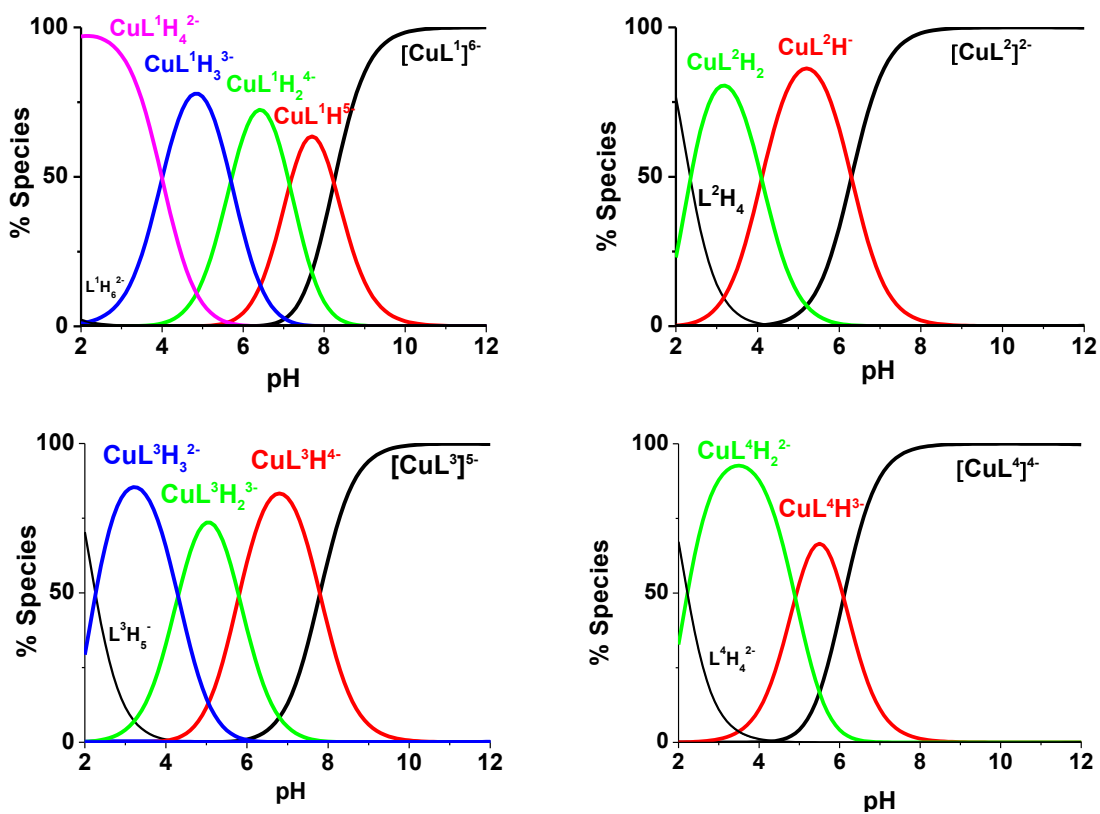


Figure S2. Distribution diagrams as a function of pH of the protonated cupric complexes formed with ligands L^1 , L^2 , L^3 and L^4 . Solvent: H_2O ; $T = 25.0(2) \text{ } ^\circ\text{C}$; $I = 0.1 \text{ M}$ ($NaClO_4$). $[L] = [Cu] = 2 \times 10^{-3} \text{ M}$.

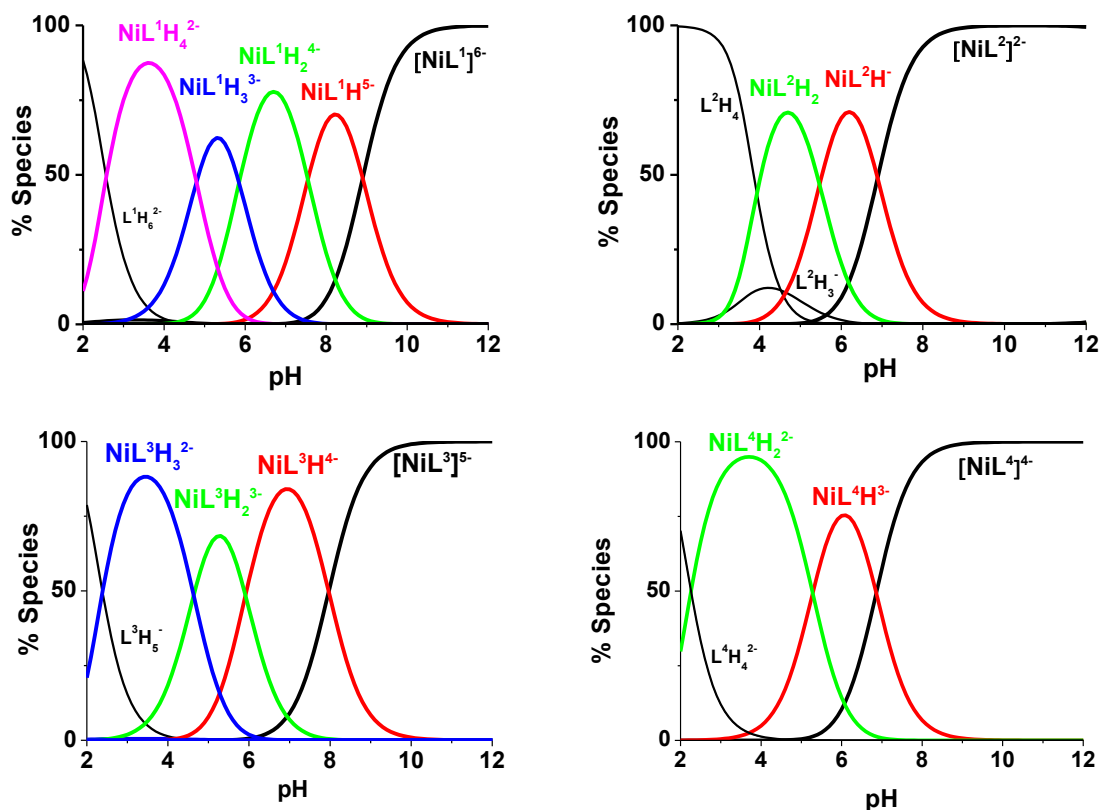


Figure S3. Distribution diagrams as a function of pH of the protonated nickel(II) complexes formed with ligands **L¹**, **L²**, **L³** and **L⁴**. Solvent: H₂O; *T* = 25.0(2) °C; *I* = 0.1 M (NaClO₄). [**L**] = [Ni] = 2 × 10⁻³ M.

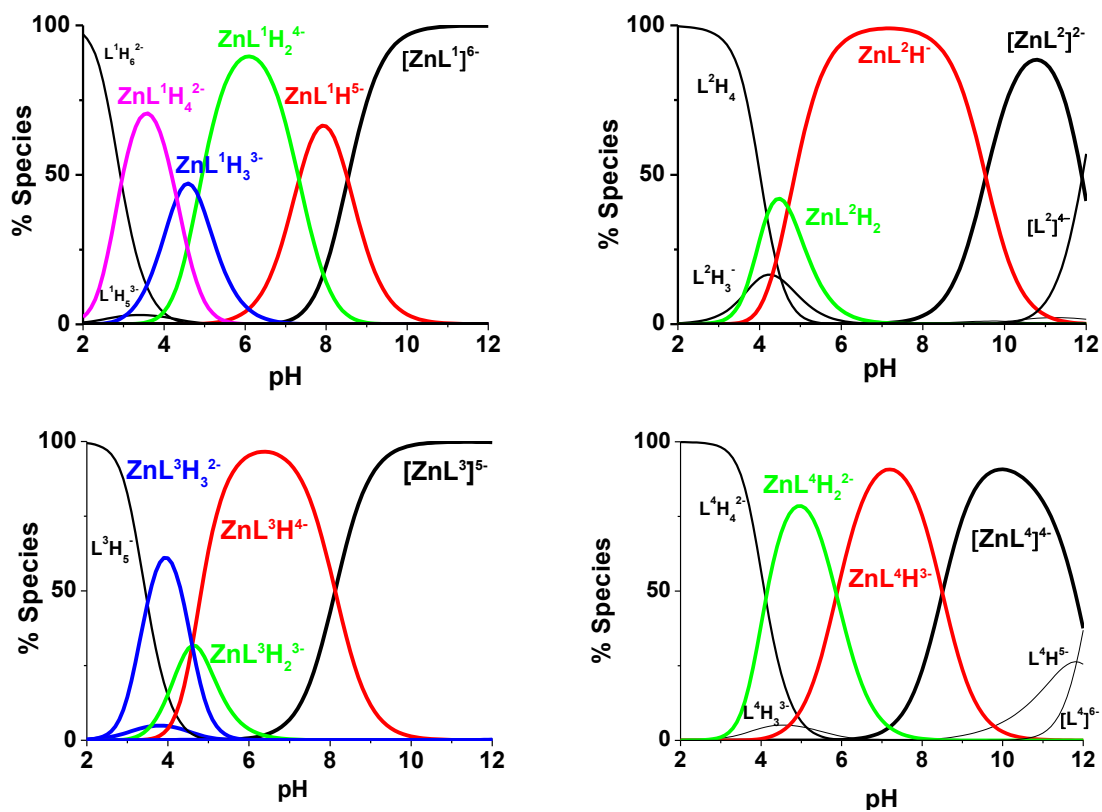


Figure S4. Distribution diagrams as a function of pH of the protonated zinc(II) complexes formed with ligands **L¹**, **L²**, **L³** and **L⁴**. Solvent: H₂O; *T* = 25.0(2) °C; *I* = 0.1 M (NaClO₄). [**L**] = [Zn] = 2 × 10⁻³ M.

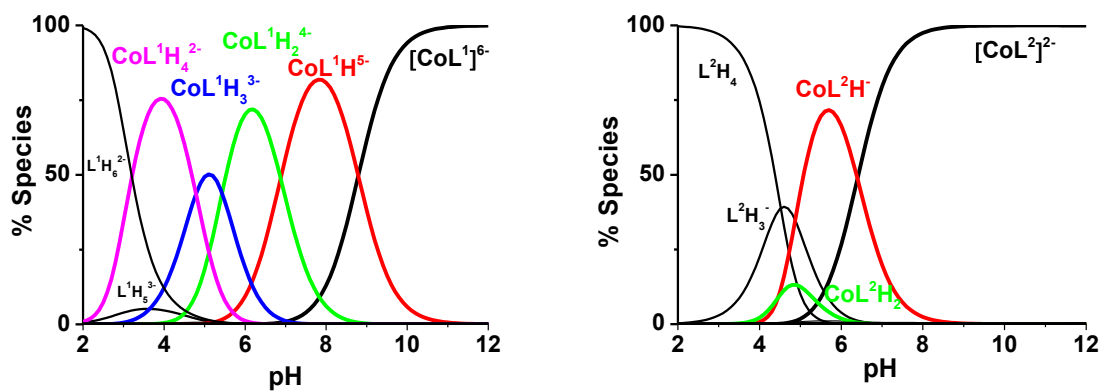


Figure S5. Distribution diagrams as a function of pH of the protonated cobalt(II) complexes formed with ligands L^1 and L^2 . Solvent: H_2O ; $T = 25.0(2) \text{ }^\circ\text{C}$; $I = 0.1 \text{ M}$ ($NaClO_4$). $[L] = [Co] = 2 \times 10^{-3} \text{ M}$.

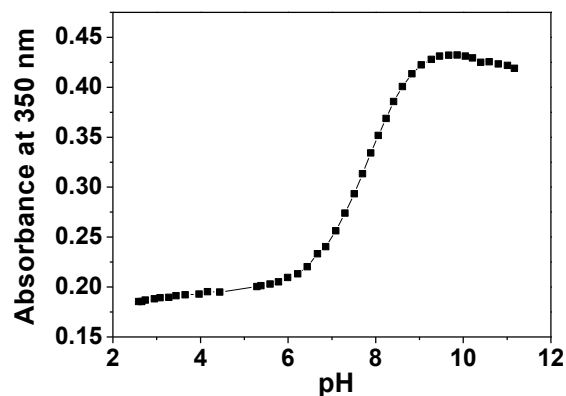
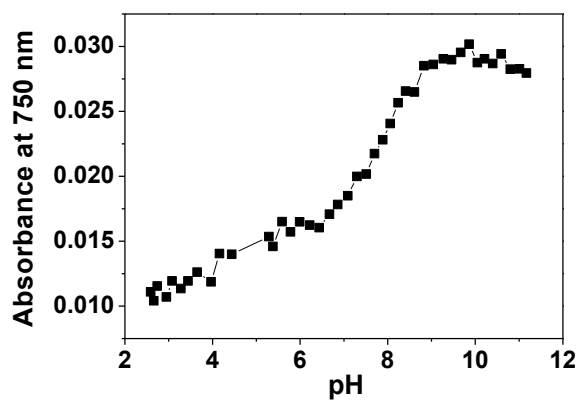
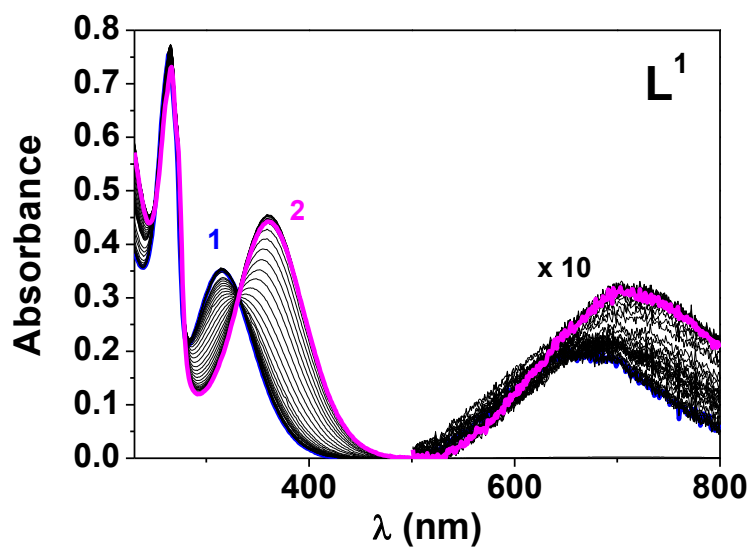
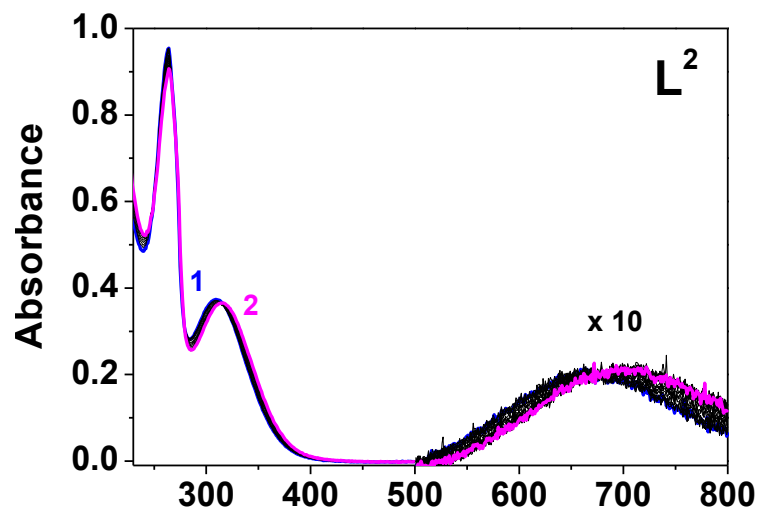


Figure S6. Absorption vs. pH titration of the cupric complexes formed with L^1 and absorbances at 350 and 750 nm as a function of pH. Solvent: H_2O ; $I = 0.1$ M ($NaClO_4$); $T = 25.0(2)$ °C; $l = 1$ cm. $[L^1]_{tot} = 1.41 \times 10^{-4}$ M ; $[Cu(II)]_{tot} = 1.40 \times 10^{-4}$ M; (1) pH = 2.59; (2) pH = 11.17.



(a)

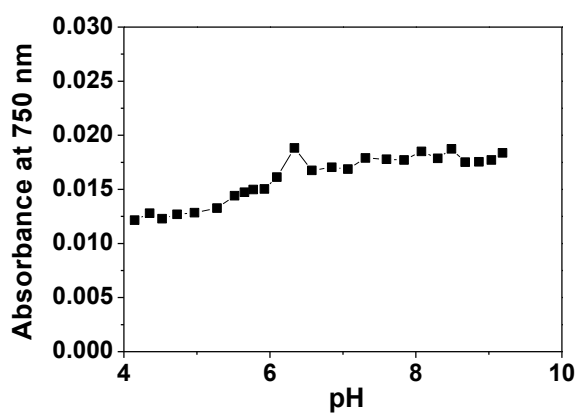
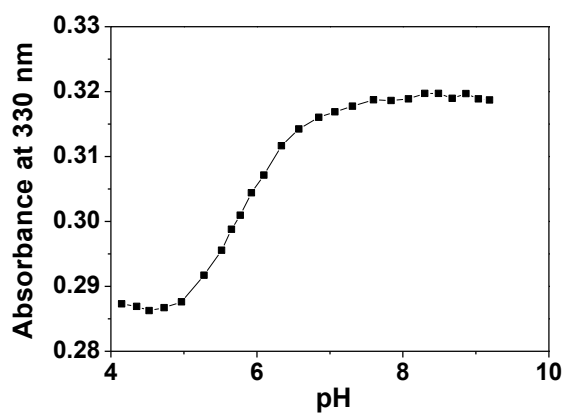


Figure S7. Absorption vs. pH titrations of the cupric complexes formed with L^2 and absorbances at 350 and 750 nm as a function of pH. Solvent: H_2O ; $I = 0.1$ M ($NaClO_4$); $T = 25.0(2)$ °C; $l = 1$ cm. $[L^2]_{tot} = 1.39 \times 10^{-4}$ M; $[Cu(II)]_{tot} = 1.30 \times 10^{-4}$ M; (1) pH = 4.15; (2) pH = 9.19.

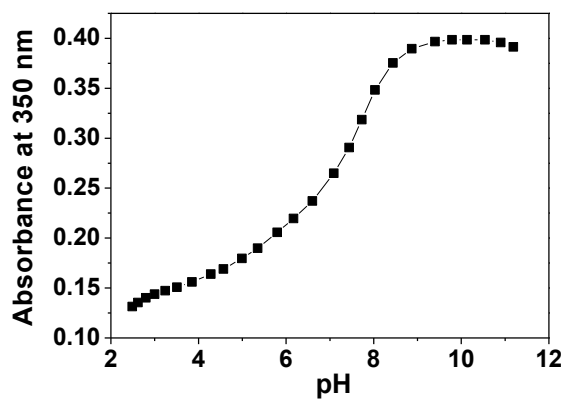
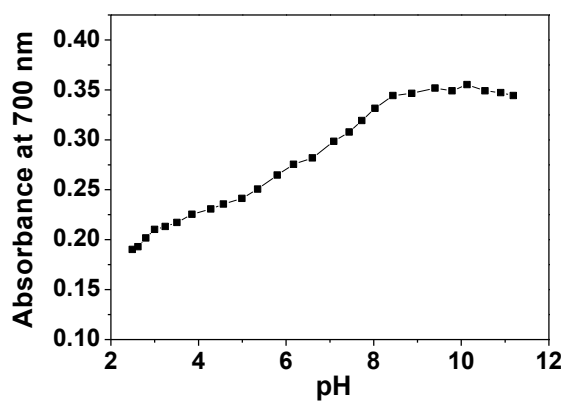
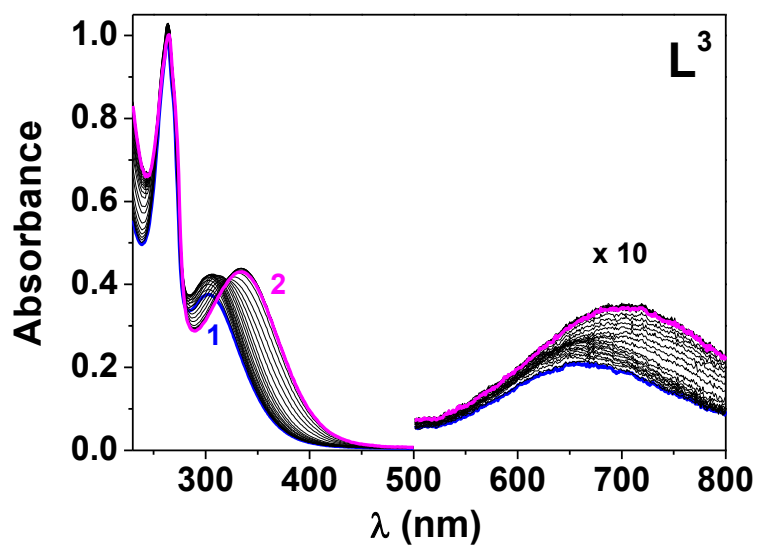
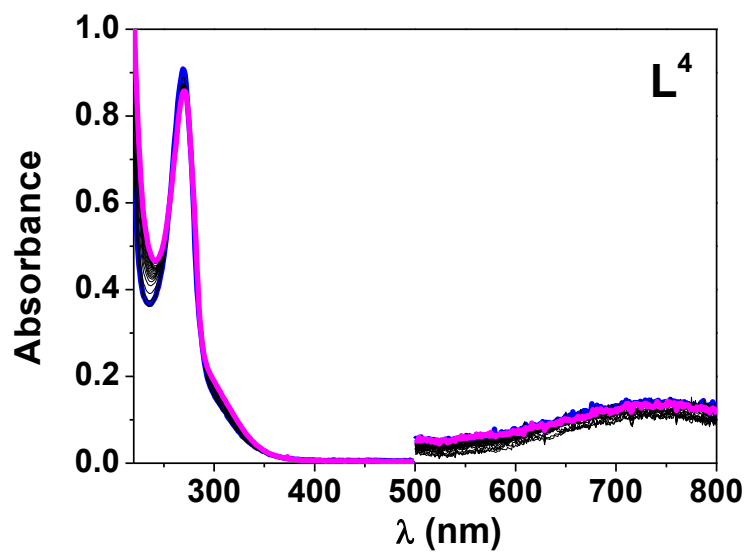


Figure S8. Absorption vs. pH titrations of the cupric complexes formed with L^3 and absorbances at 350 and 700 nm as a function of pH. Solvent: H_2O ; $I = 0.1$ M ($NaClO_4$); $T = 25.0(2)$ °C; $l = 1$ cm. $[L^3]_{tot} = [Cu(II)]_{tot} = 1.78 \times 10^{-4}$ M; (1) pH = 2.49; (2) pH = 11.19.



(b)

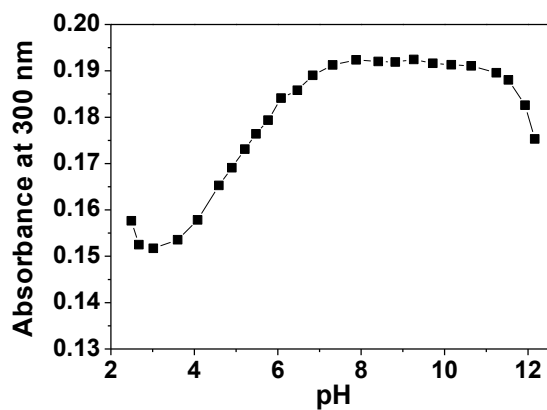
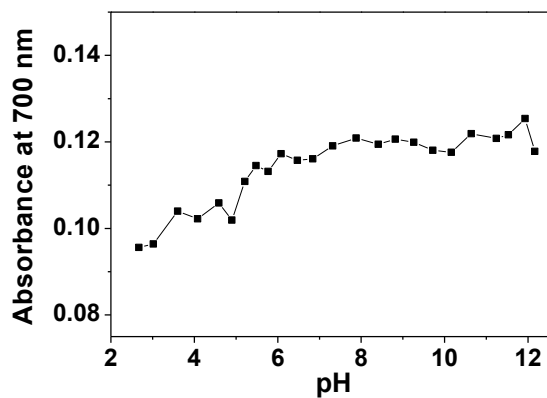
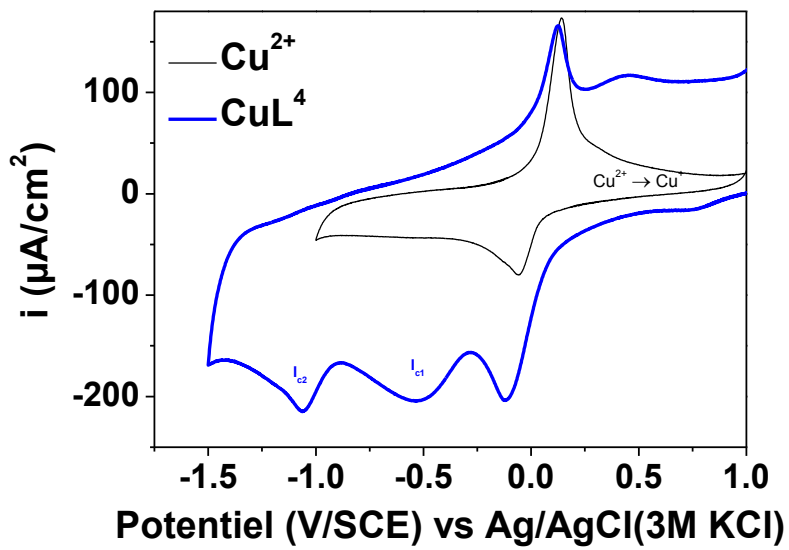
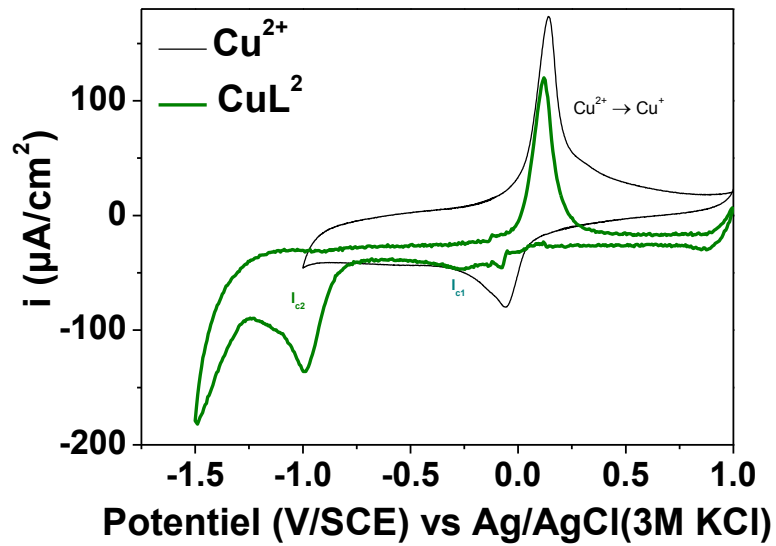
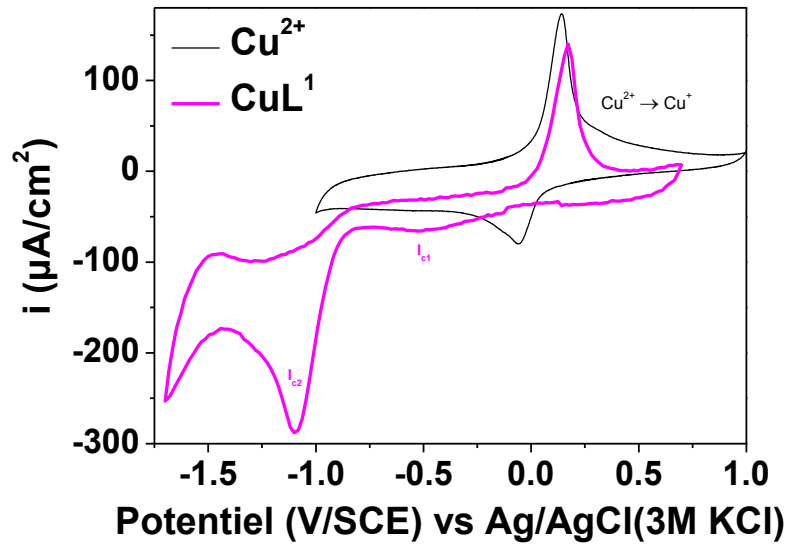


Figure S9. Absorption vs. pH titrations of the cupric complexes formed with L^4 and absorbances at 300 and 700 nm as a function of pH. Solvent: H_2O ; $I = 0.1\text{ M}$ ($NaClO_4$); $T = 25.0(2)\text{ }^\circ\text{C}$; $l = 1\text{ cm}$. $[L^3]_{\text{tot}} = [Cu(II)]_{\text{tot}} = 1.30 \times 10^{-4}\text{ M}$; (1) $pH = 2.49$; (2) $pH = 12.16$.



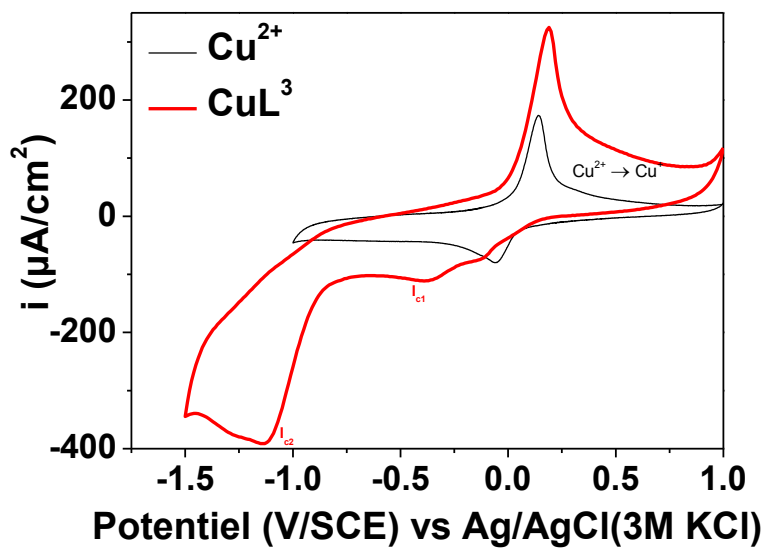
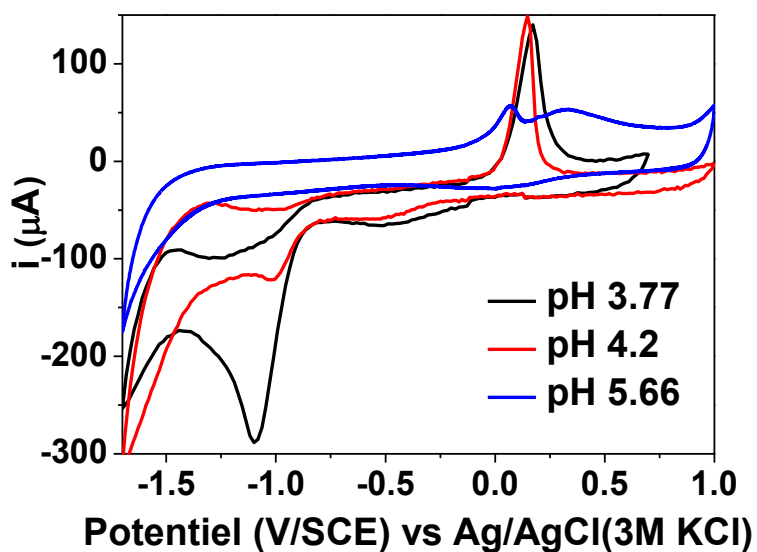


Figure S10. Cyclic voltamperograms of CuL^1 , CuL^2 , CuL^3 and CuL^4 measured in water at pH ~ 3.7 . Solvent: H_2O ; $I = 0.1 \text{ M}$ (NaClO_4); $T = 25.0(2) \text{ }^\circ\text{C}$; reference = Ag/AgCl ; $[\text{CuL}^1]_{\text{tot}} = 9.94 \times 10^{-4} \text{ M}$; $\nu = 200 \text{ mV}$.



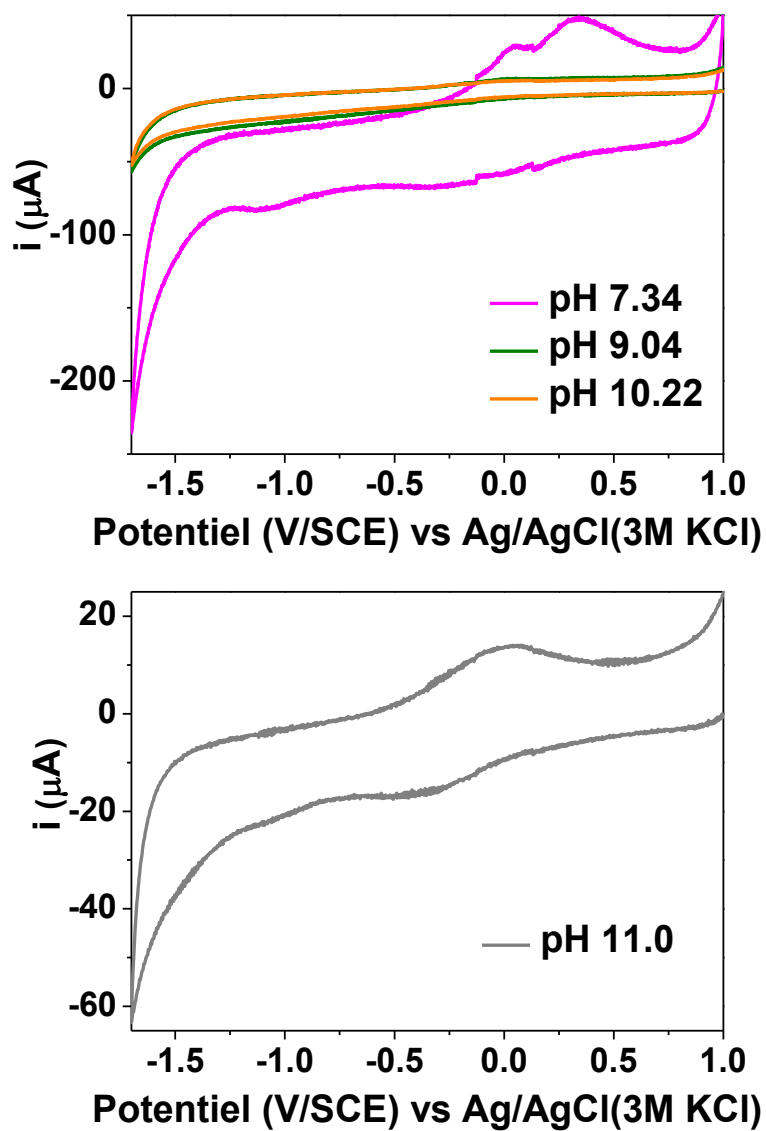


Figure S11. CV of CuL¹ as a function of pH. Solvent: H₂O; *I* = 0.1 M (NaClO₄); *T* = 25.0(2) °C; reference = Ag/AgCl; [CuL¹]_{tot} = 9.94 × 10⁻⁴ M; *v* = 200 mV.

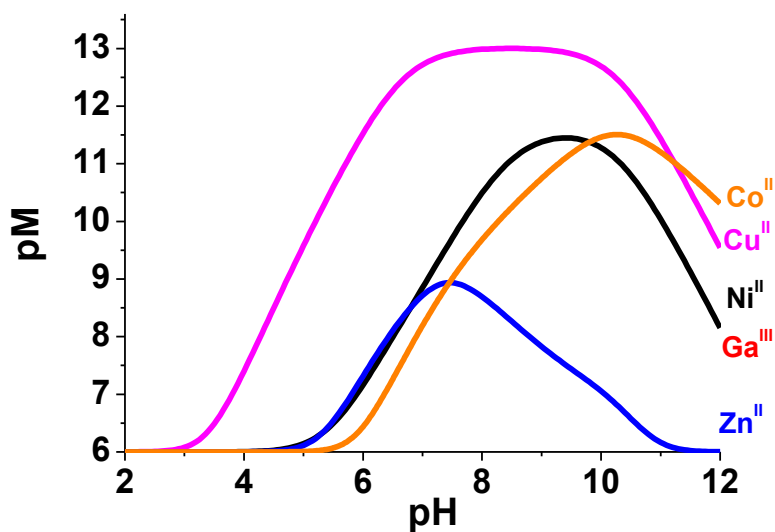


Figure S12. (a) Variation of the pM values ($M = \text{Cu}^{\text{II}}$, Zn^{II} , Ni^{II} , Co^{II} and Ga^{III}) as a function of pH for ligand L^2 . Solvent: H_2O ; $I = 0.1 \text{ M}$; $T = 25.0(2) \text{ }^\circ\text{C}$; $\text{pM} = -\log[\text{M}^{\text{II}}]_{\text{free}}$ or $-\log[\text{M}^{\text{III}}]_{\text{free}}$, $[\text{L}]_{\text{tot}} = 10^{-5} \text{ M}$ and $[\text{M}^{\text{II}}]_{\text{tot}}$ or $[\text{M}^{\text{III}}]_{\text{tot}} = 10^{-6} \text{ M}$.

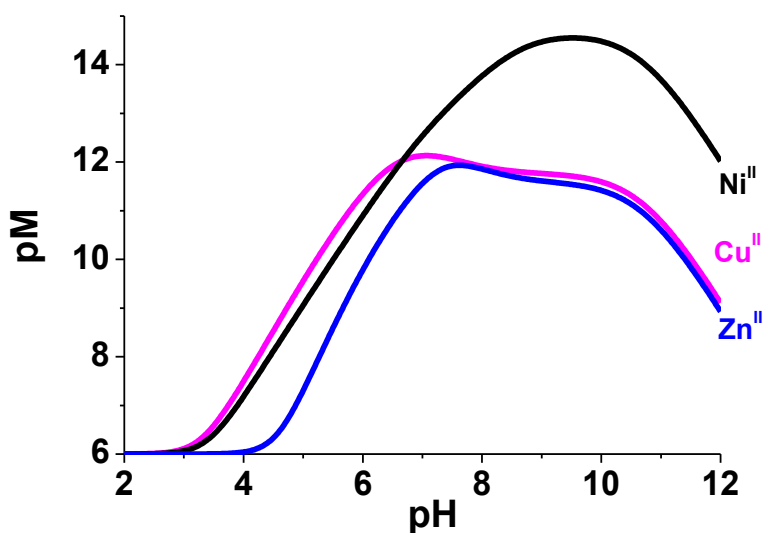


Figure S13. (a) Variation of the pM values ($M = \text{Cu}^{\text{II}}$, Zn^{II} , Ni^{II}) as a function of pH for ligand L^3 . Solvent: H_2O ; $I = 0.1 \text{ M}$; $T = 25.0(2) \text{ }^\circ\text{C}$; $\text{pM} = -\log[\text{M}^{\text{II}}]_{\text{free}}$ or $-\log[\text{M}^{\text{III}}]_{\text{free}}$, $[\text{L}]_{\text{tot}} = 10^{-5} \text{ M}$ and $[\text{M}^{\text{II}}]_{\text{tot}}$ or $[\text{M}^{\text{III}}]_{\text{tot}} = 10^{-6} \text{ M}$.

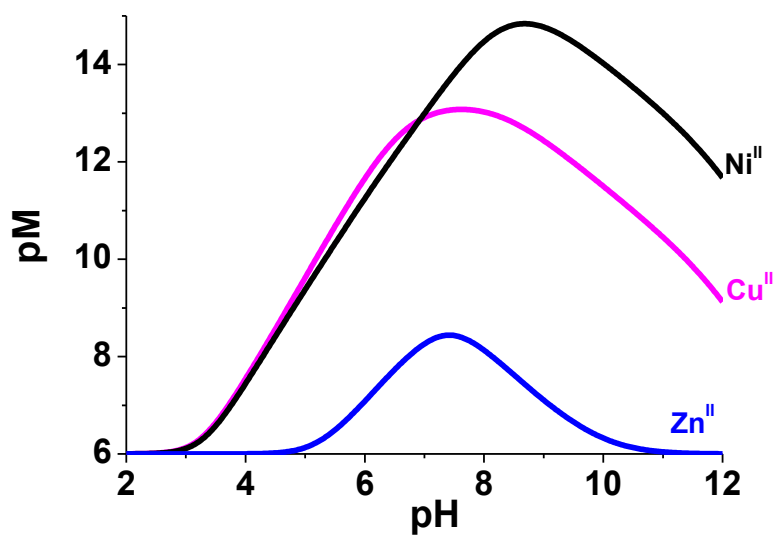


Figure S14. (a) Variation of the pM values ($M = \text{Cu}^{\text{II}}, \text{Zn}^{\text{II}}, \text{Ni}^{\text{II}}$) as a function of pH for ligand L^4 . Solvent: H_2O ; $I = 0.1 \text{ M}$; $T = 25.0(2) \text{ }^\circ\text{C}$; $\text{pM} = -\log[\text{M}^{\text{II}}]_{\text{free}}$ or $-\log[\text{M}^{\text{III}}]_{\text{free}}$, $[\text{L}]_{\text{tot}} = 10^{-5} \text{ M}$ and $[\text{M}^{\text{II}}]_{\text{tot}}$ or $[\text{M}^{\text{III}}]_{\text{tot}} = 10^{-6} \text{ M}$.

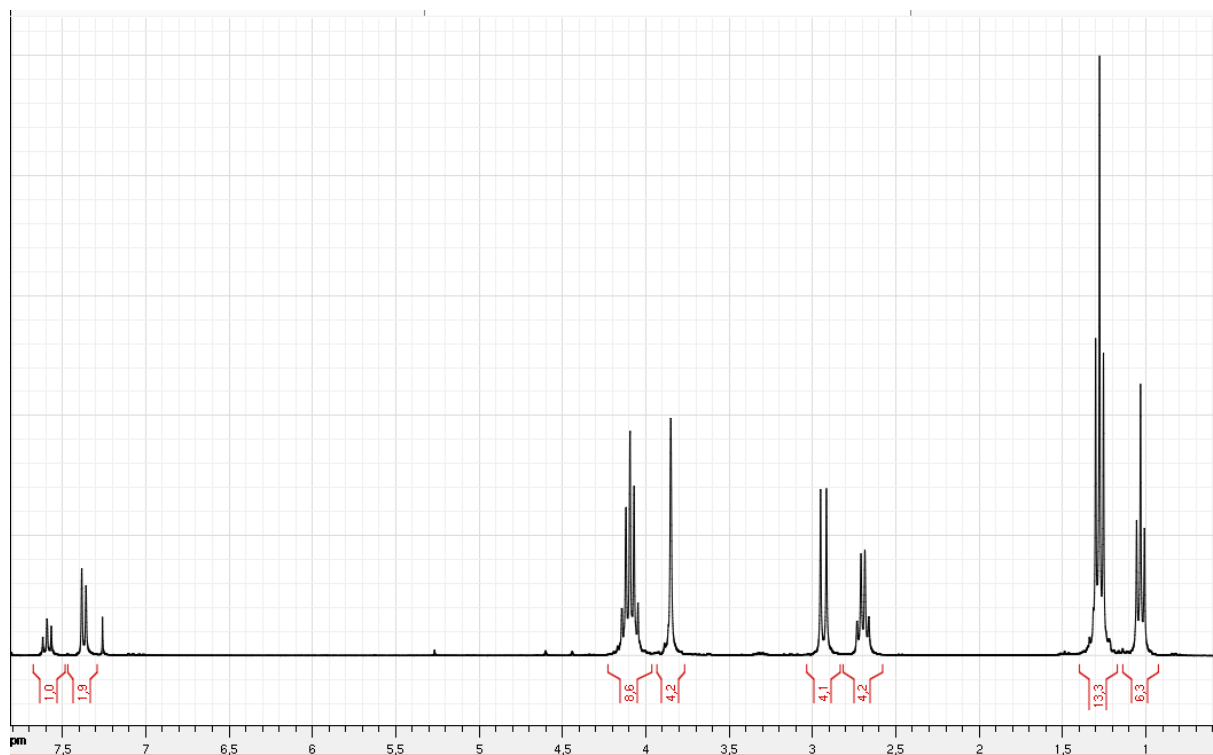


Figure S15. ¹H-NMR spectrum of compound **4** (CDCl₃, 300 MHz).

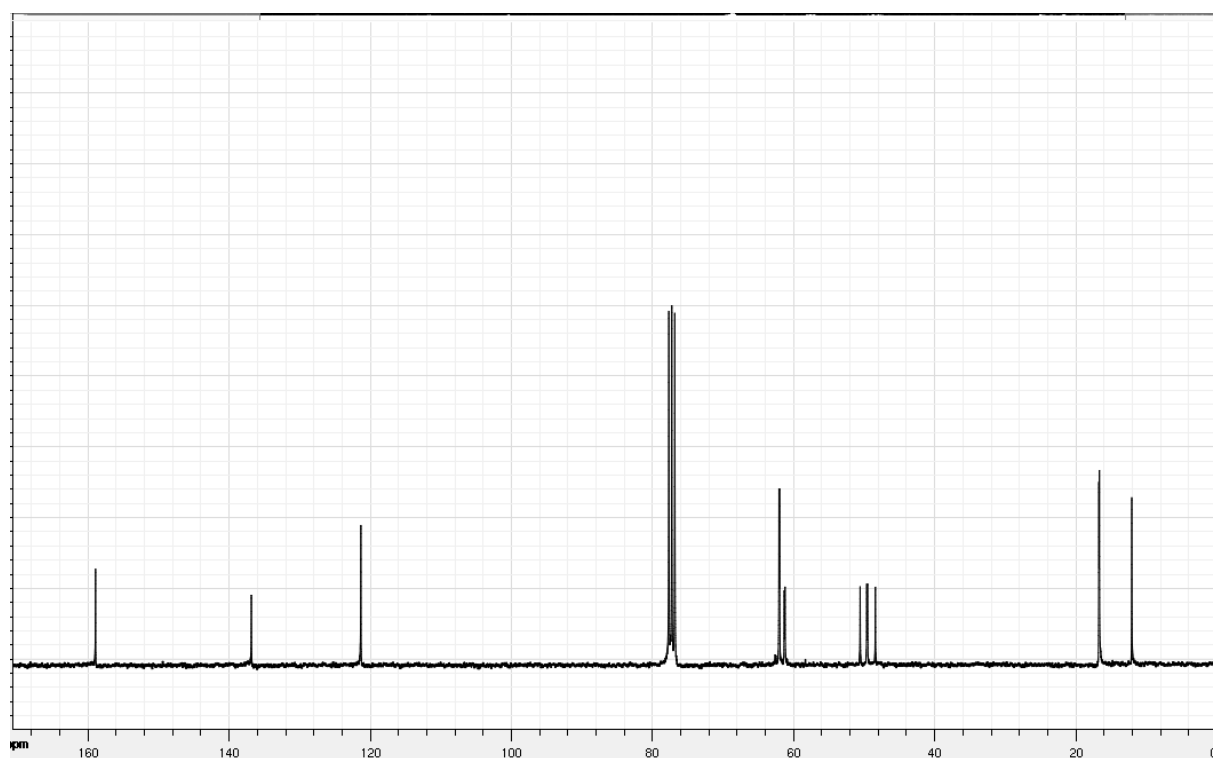


Figure S16. ¹³C-NMR spectrum of compound **4** (CDCl₃, 75 MHz).

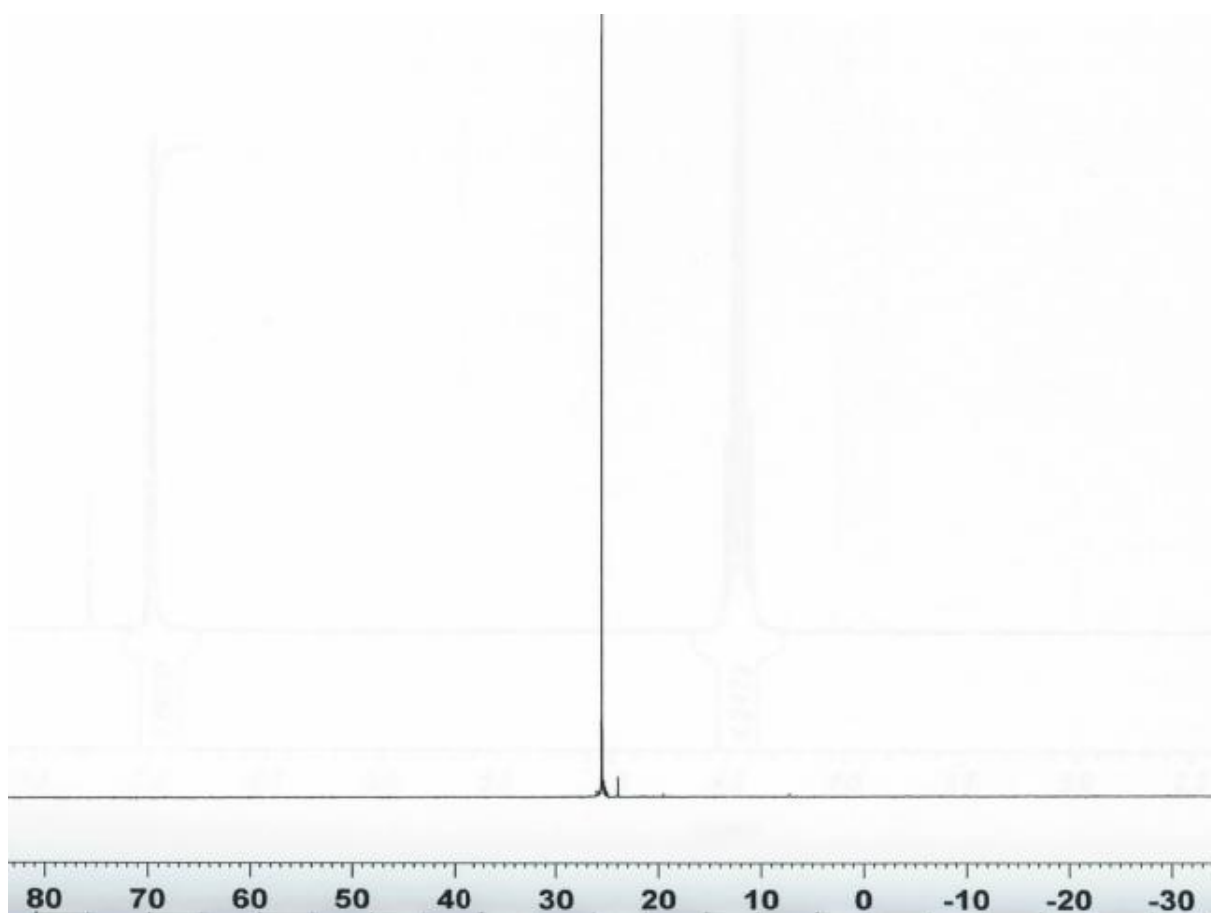


Figure S17. ^{31}P -NMR spectrum of compound **4** (CDCl_3 , 161.9 MHz).

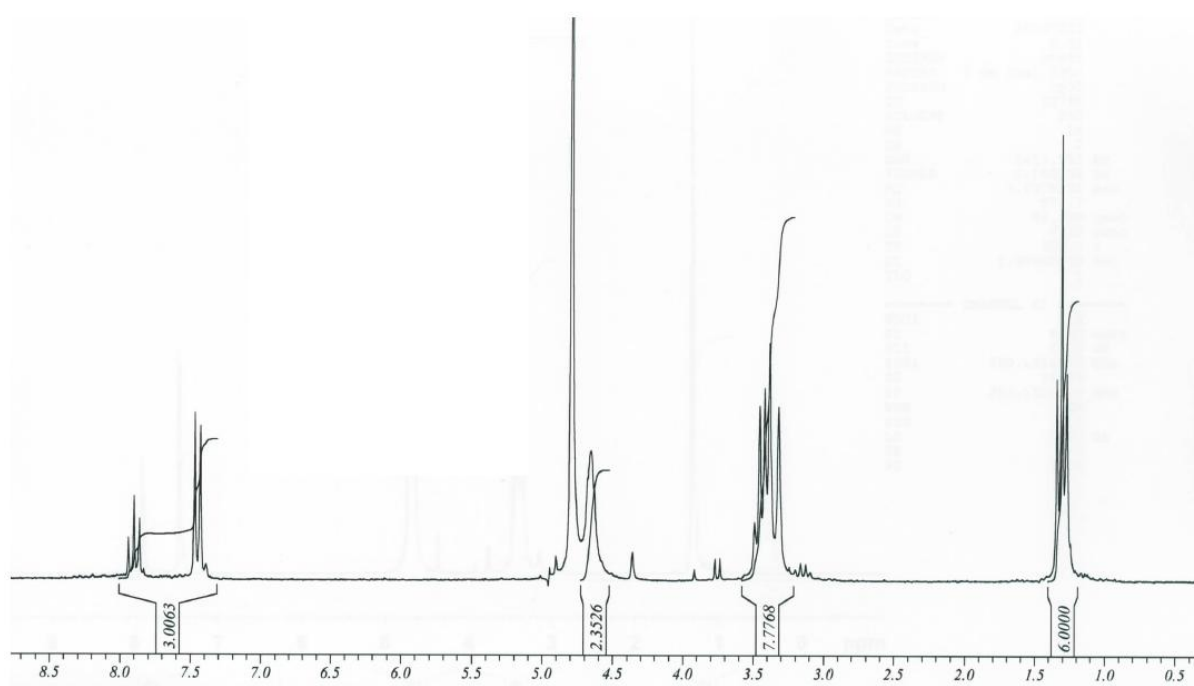


Figure S18. ^1H -NMR spectrum of Ligand **L²** (D_2O , 200 MHz)

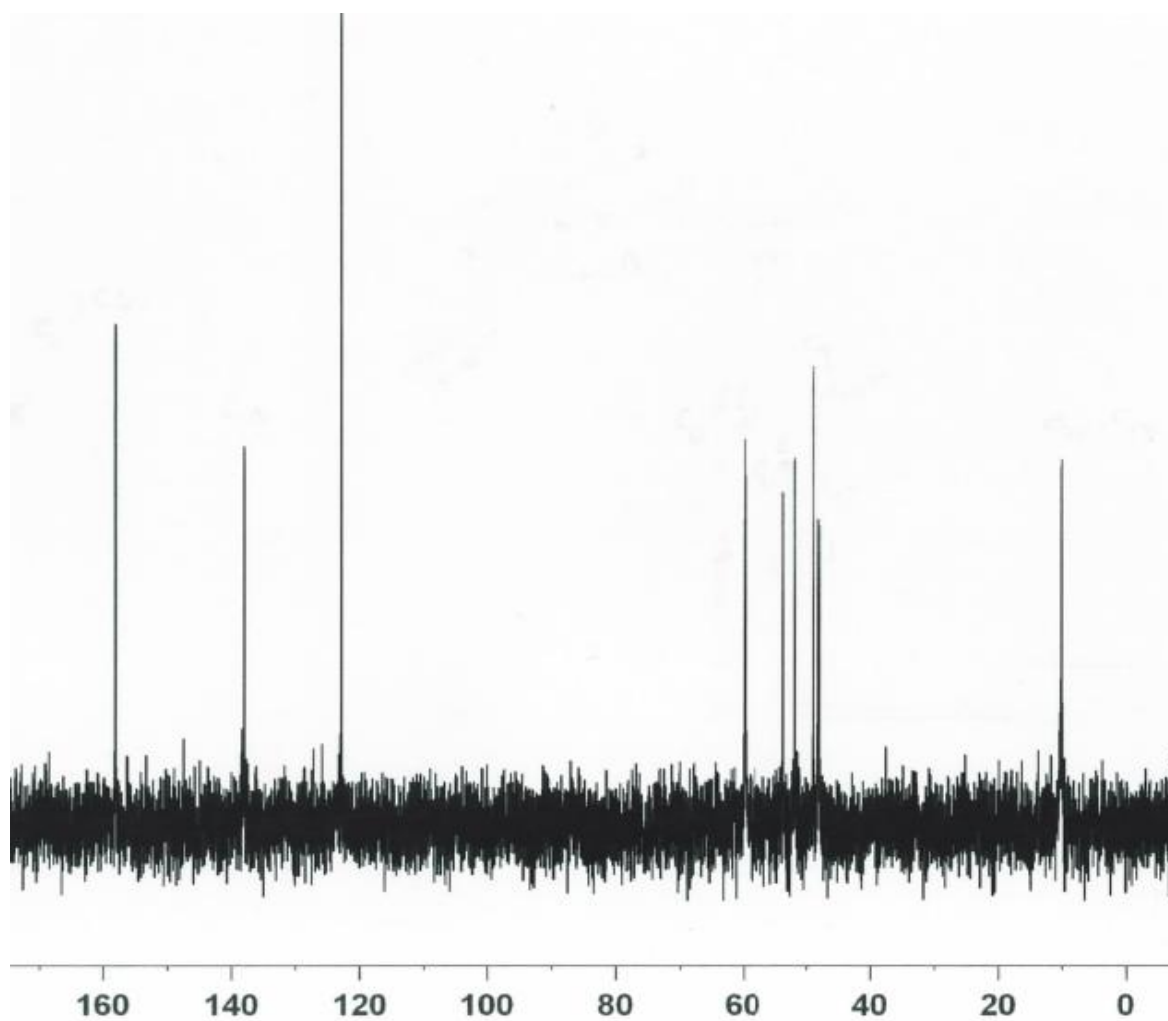


Figure S19. ^{13}C -NMR spectrum of Ligand L^2 (D_2O , 75 MHz).

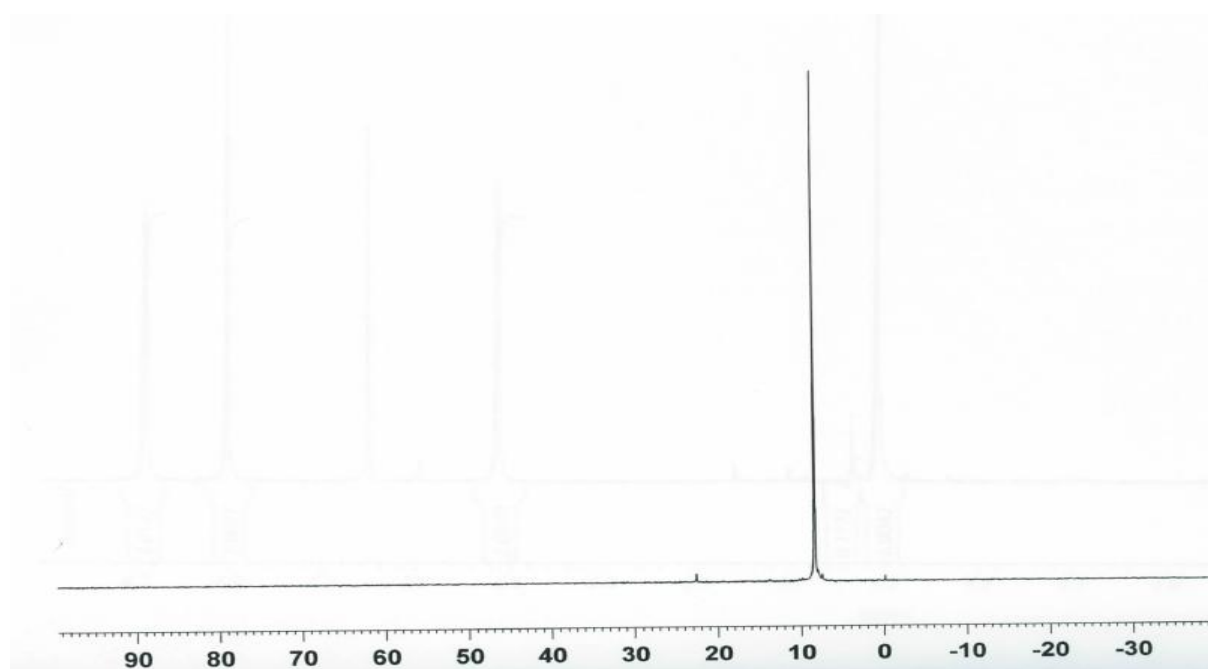


Figure S20. ^{31}P -NMR spectrum of Ligand L^2 (D_2O , 200 MHz).

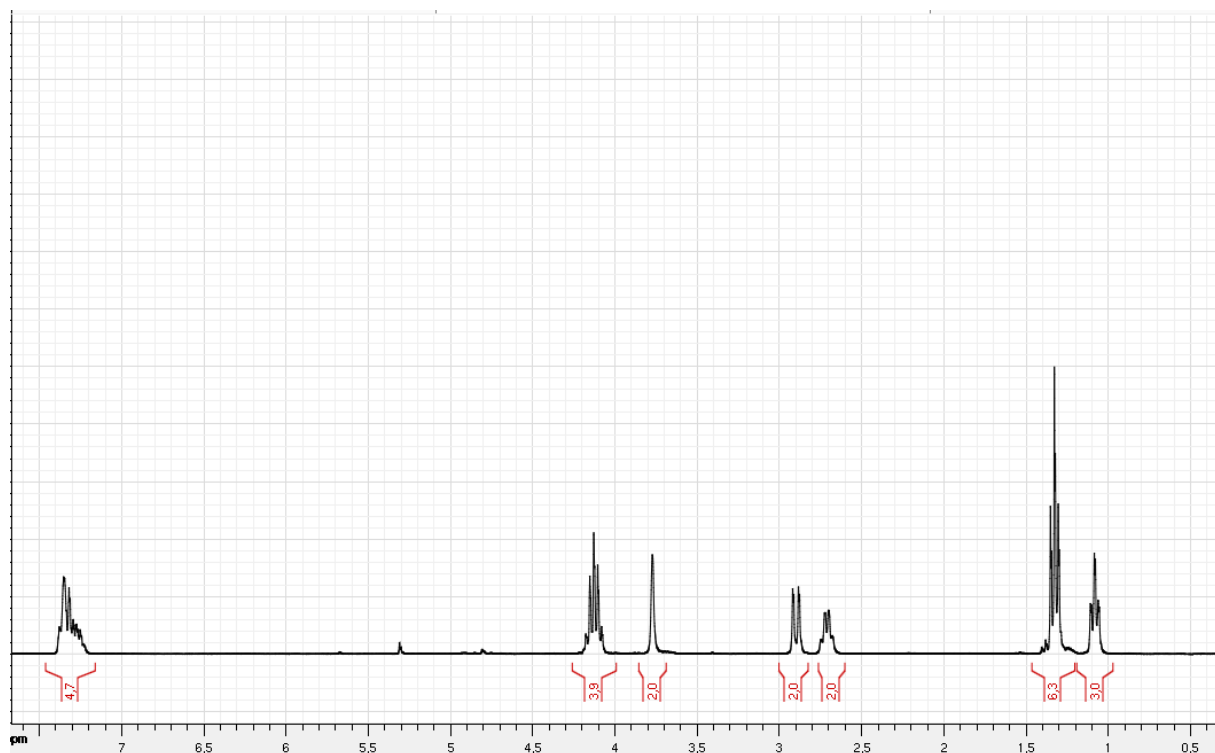


Figure S21. ^1H -NMR spectrum of compound **6** (CDCl_3 , 300 MHz).

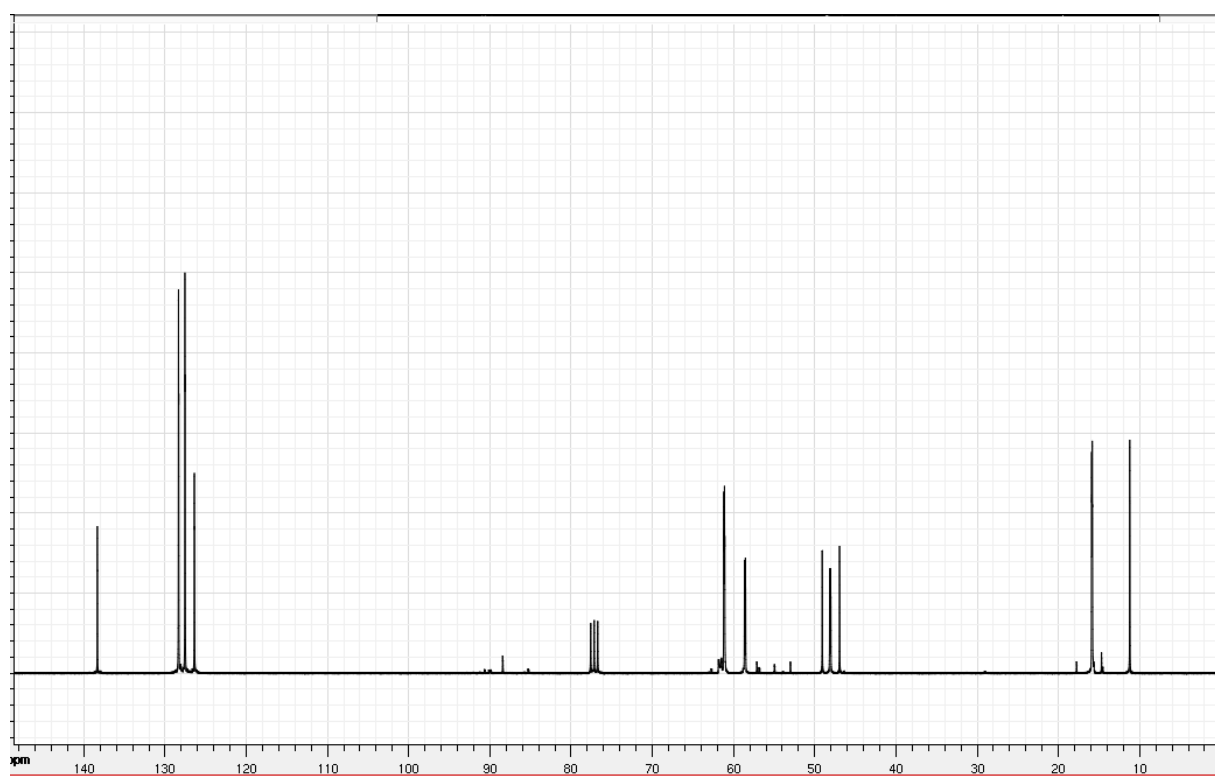


Figure S22. ^{13}C -NMR spectrum of compound **6** (CDCl_3 , 75 MHz).

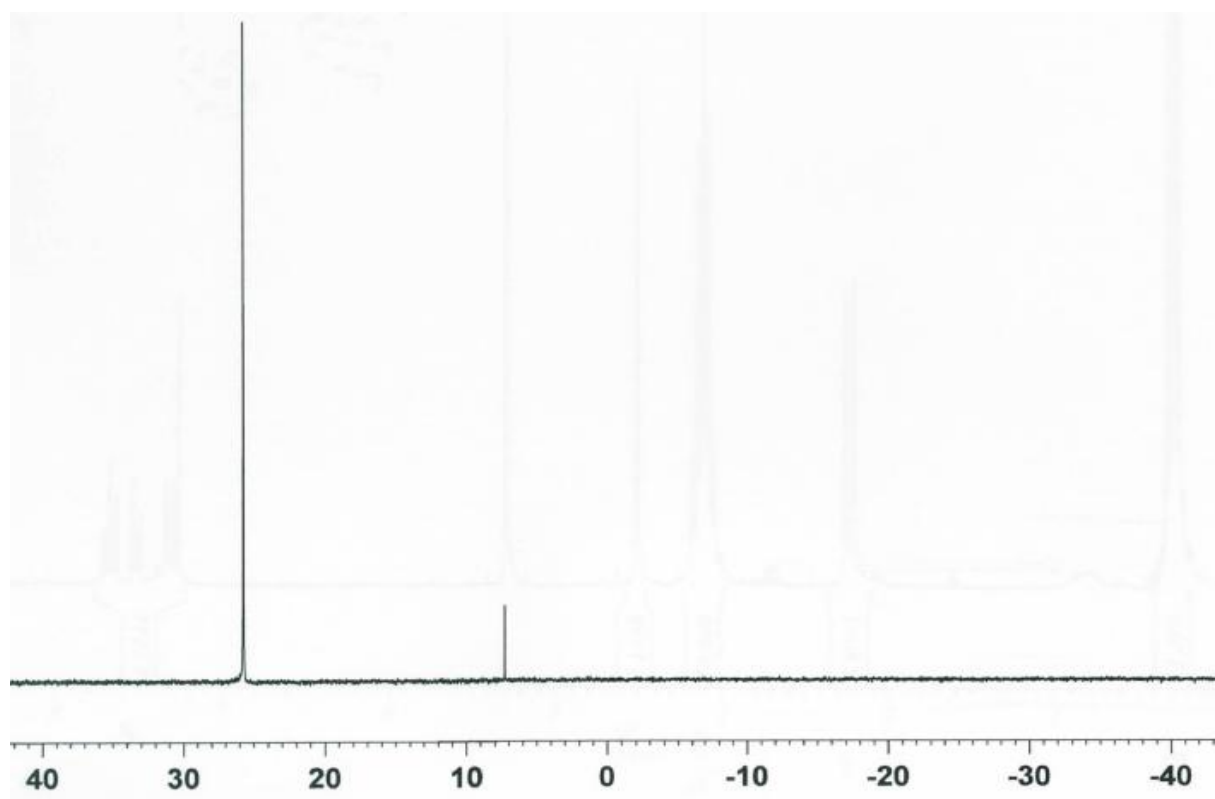


Figure S23. ^{31}P -NMR spectrum of compound **6** (CDCl_3 , 161.9 MHz).

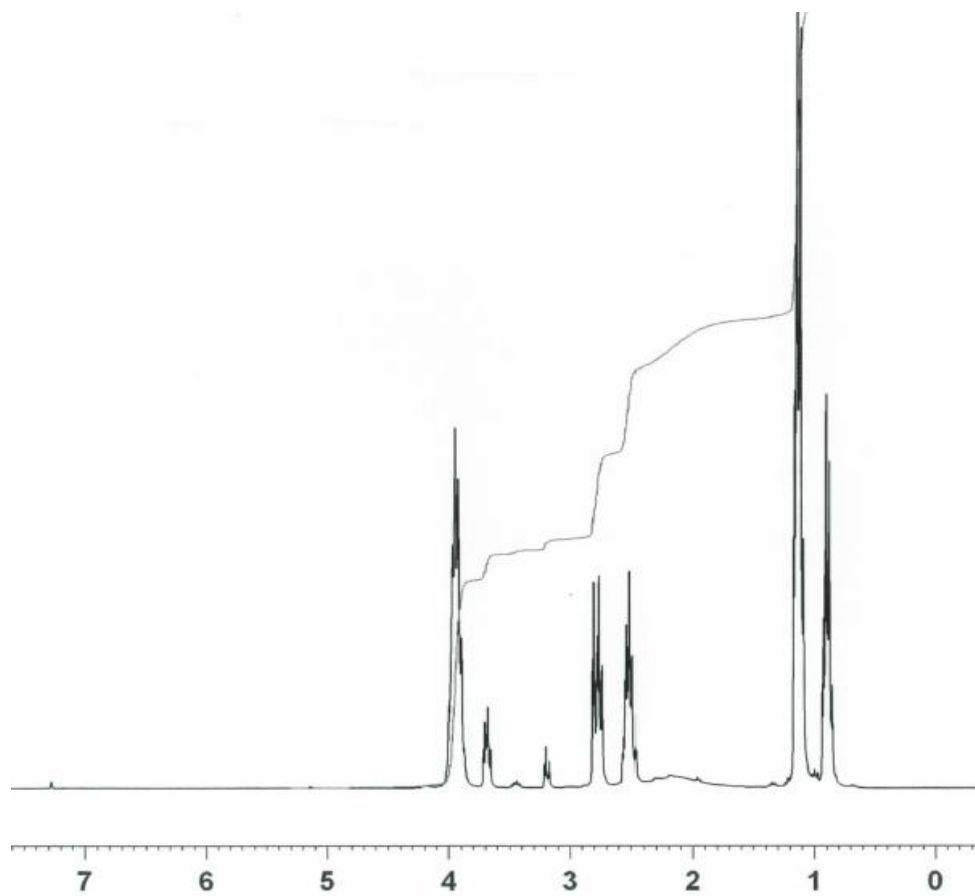


Figure S24. ^1H -NMR spectrum of compound **7** (CDCl_3 , 300 MHz).

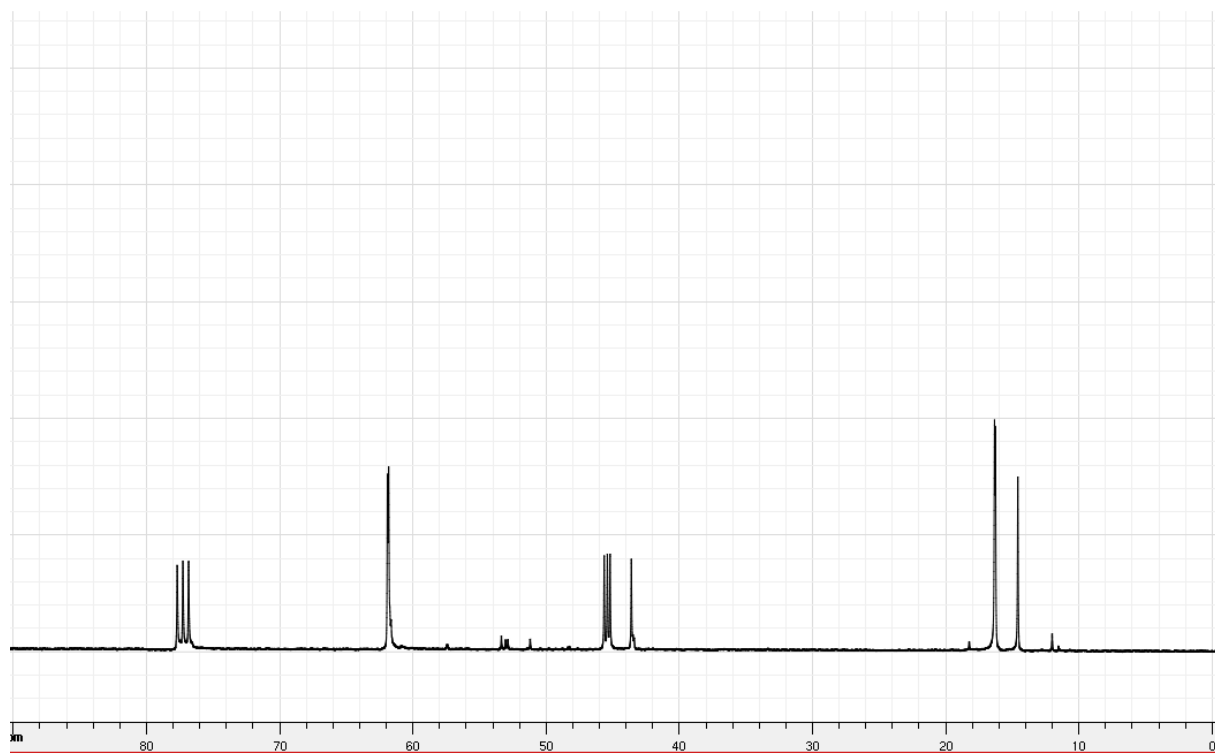


Figure S25. ^{13}C -NMR spectrum of compound **7** (CDCl_3 , 75 MHz).

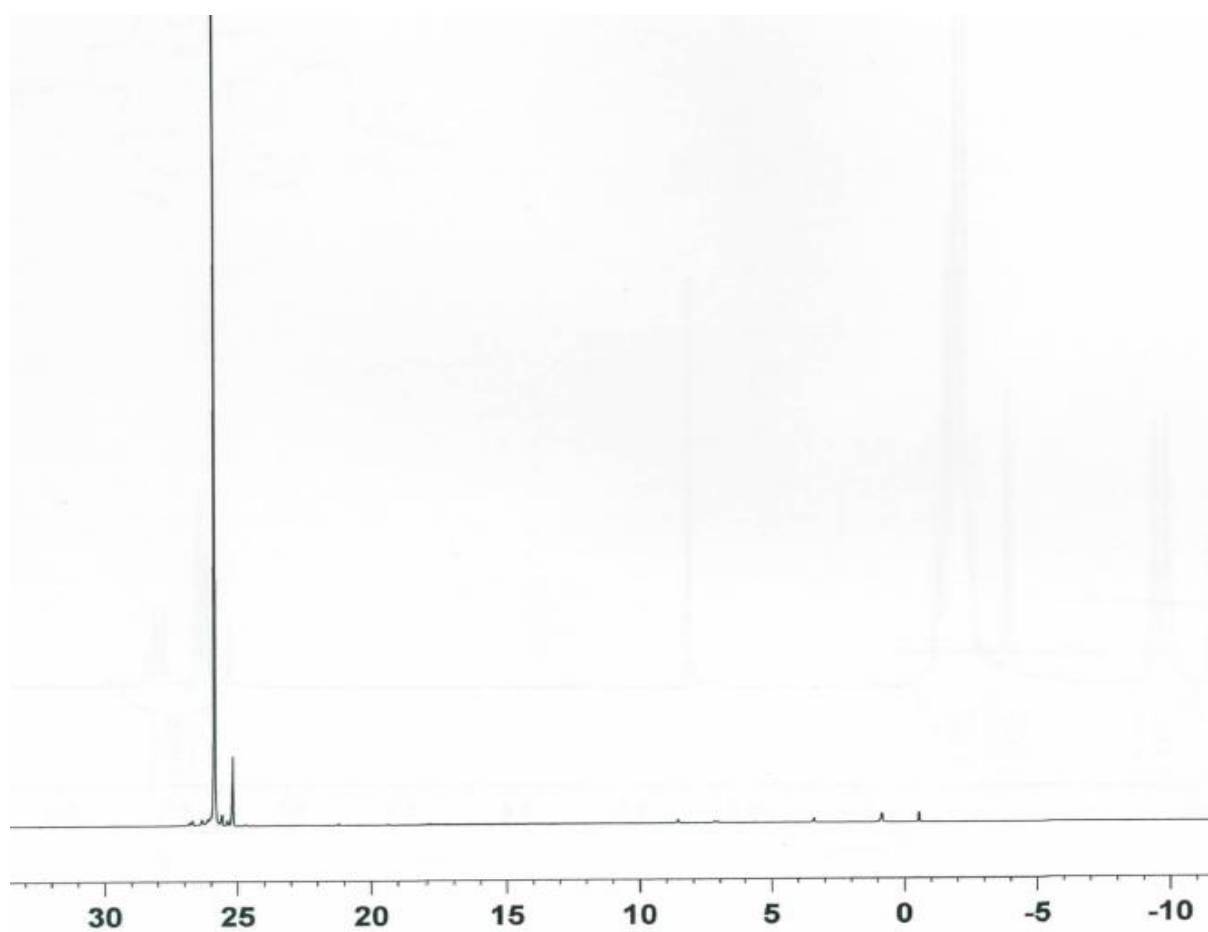


Figure S26. ^{31}P -NMR spectrum of compound **7** (CDCl_3 , 161.9 MHz).

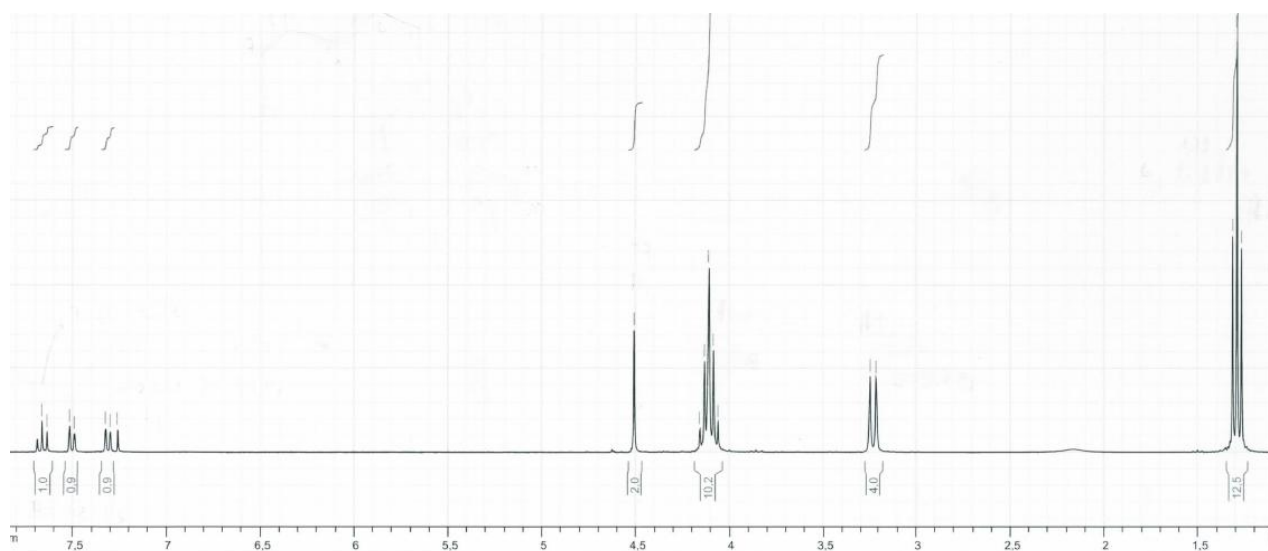


Figure S27. ^1H -NMR spectrum of compound **8** (CDCl_3 , 300 MHz).

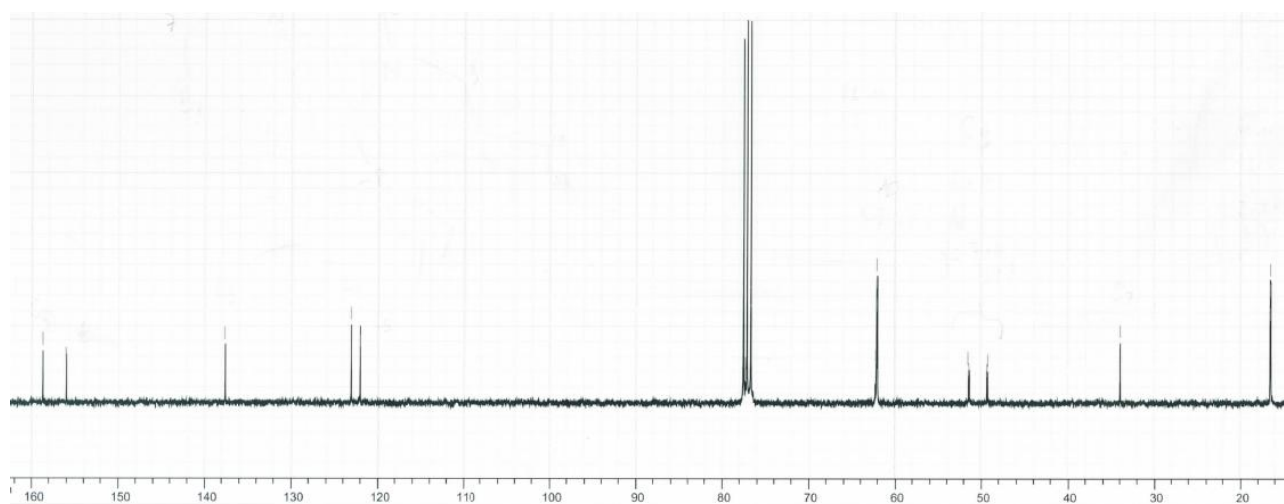


Figure S28. ^{13}C -NMR spectrum of compound **8** (CDCl_3 , 75 MHz).

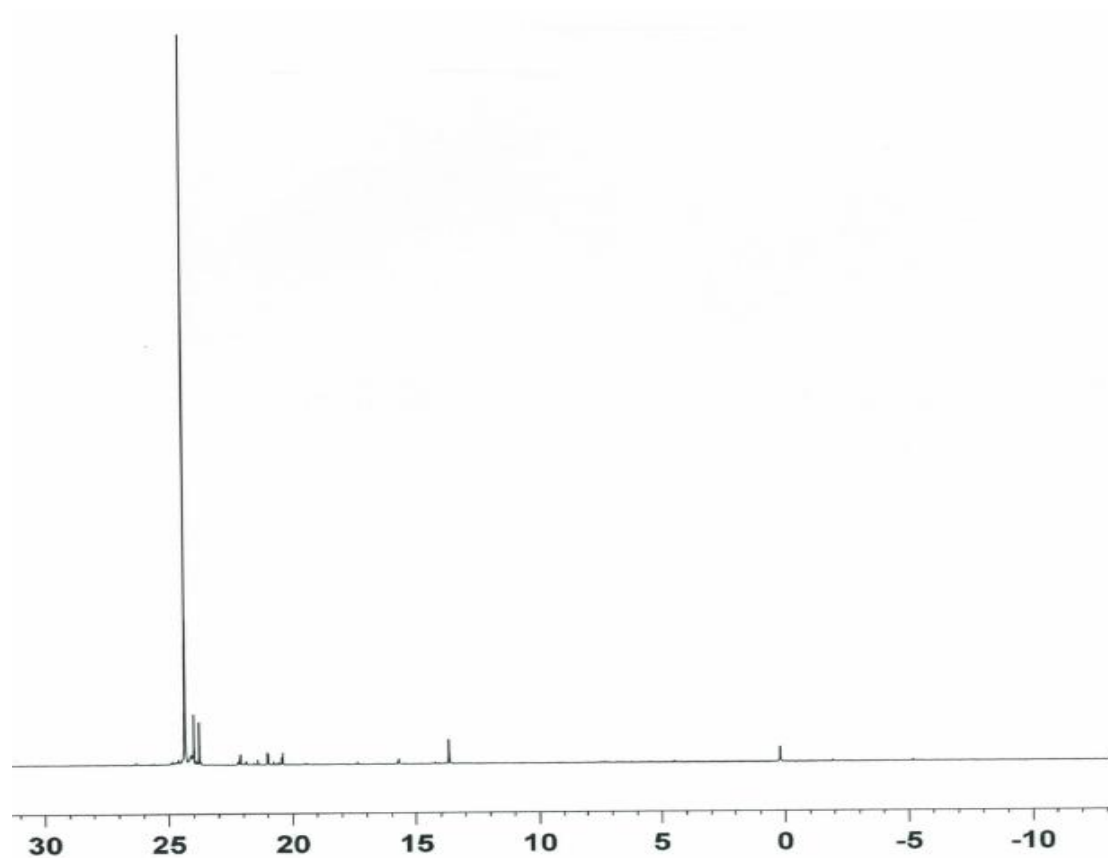


Figure S29. ^{31}P -NMR spectrum of compound **8** (CDCl_3 , 161.9 MHz).

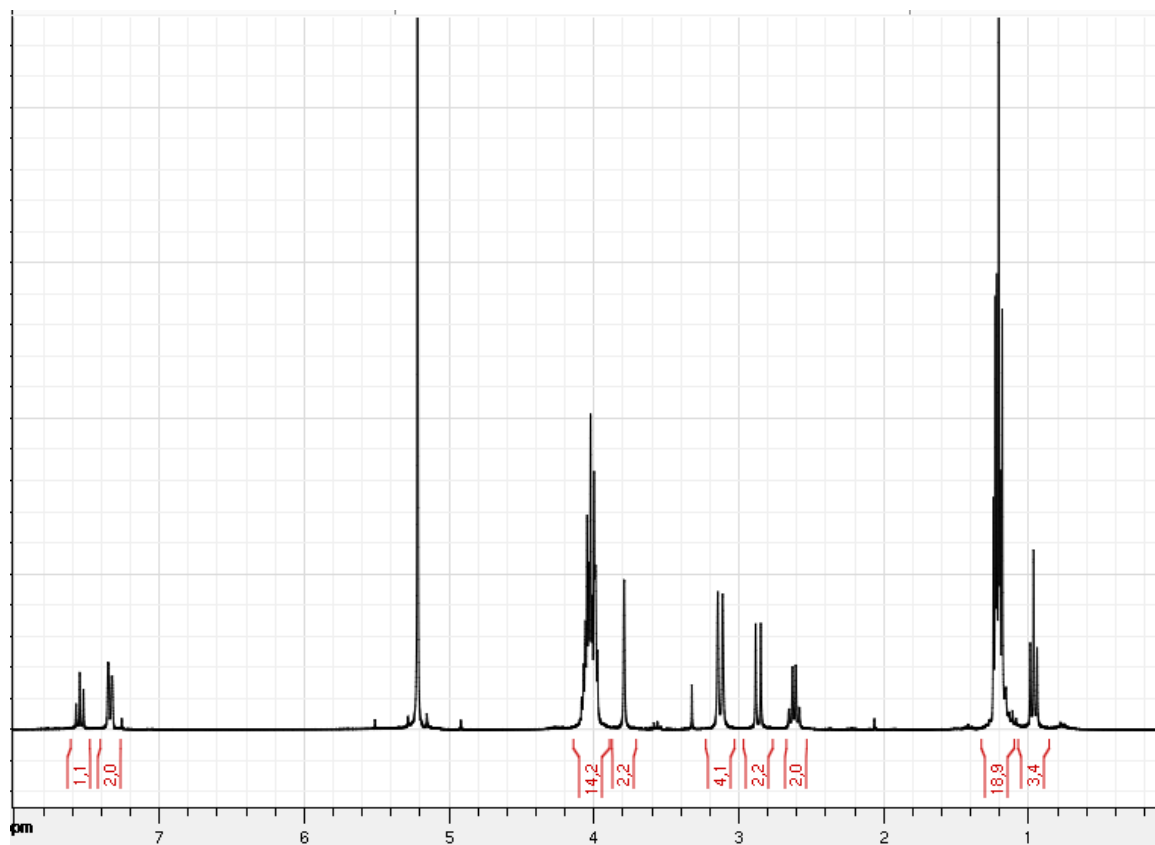


Figure S30. ^1H -NMR spectrum of compound **9** (CDCl_3 , 300 MHz).

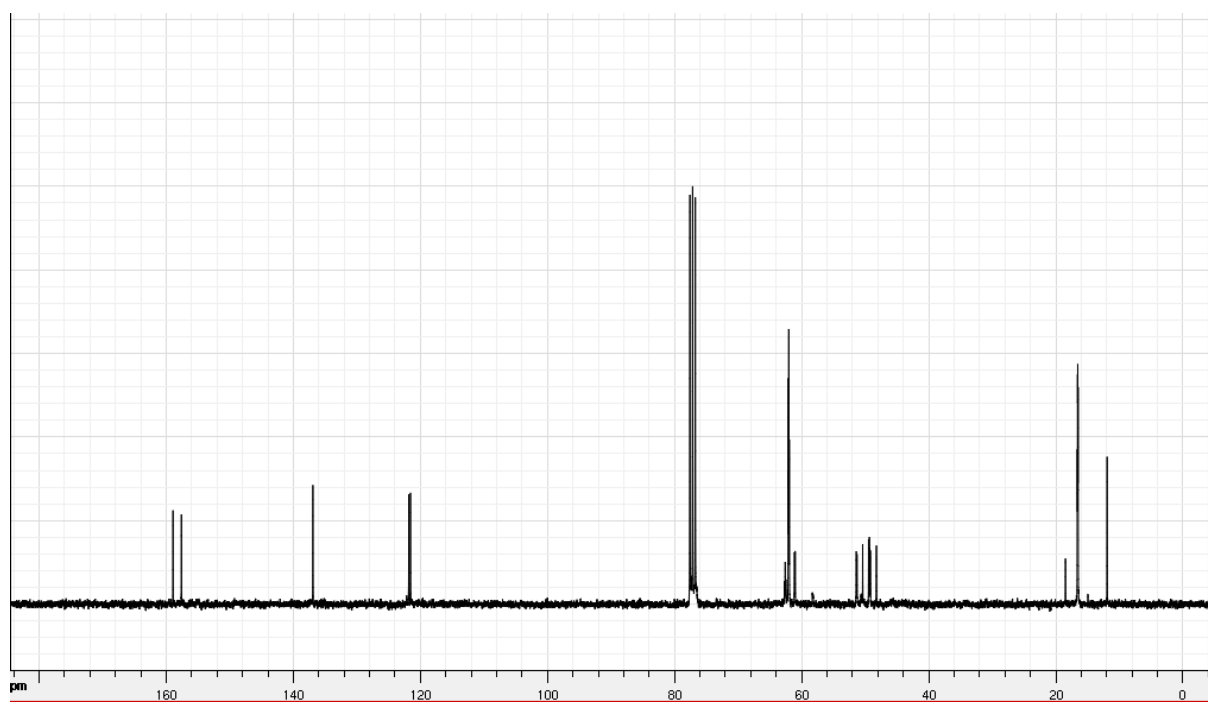


Figure S31. ^{13}C -NMR spectrum of compound **9** (CDCl_3 , 75 MHz).

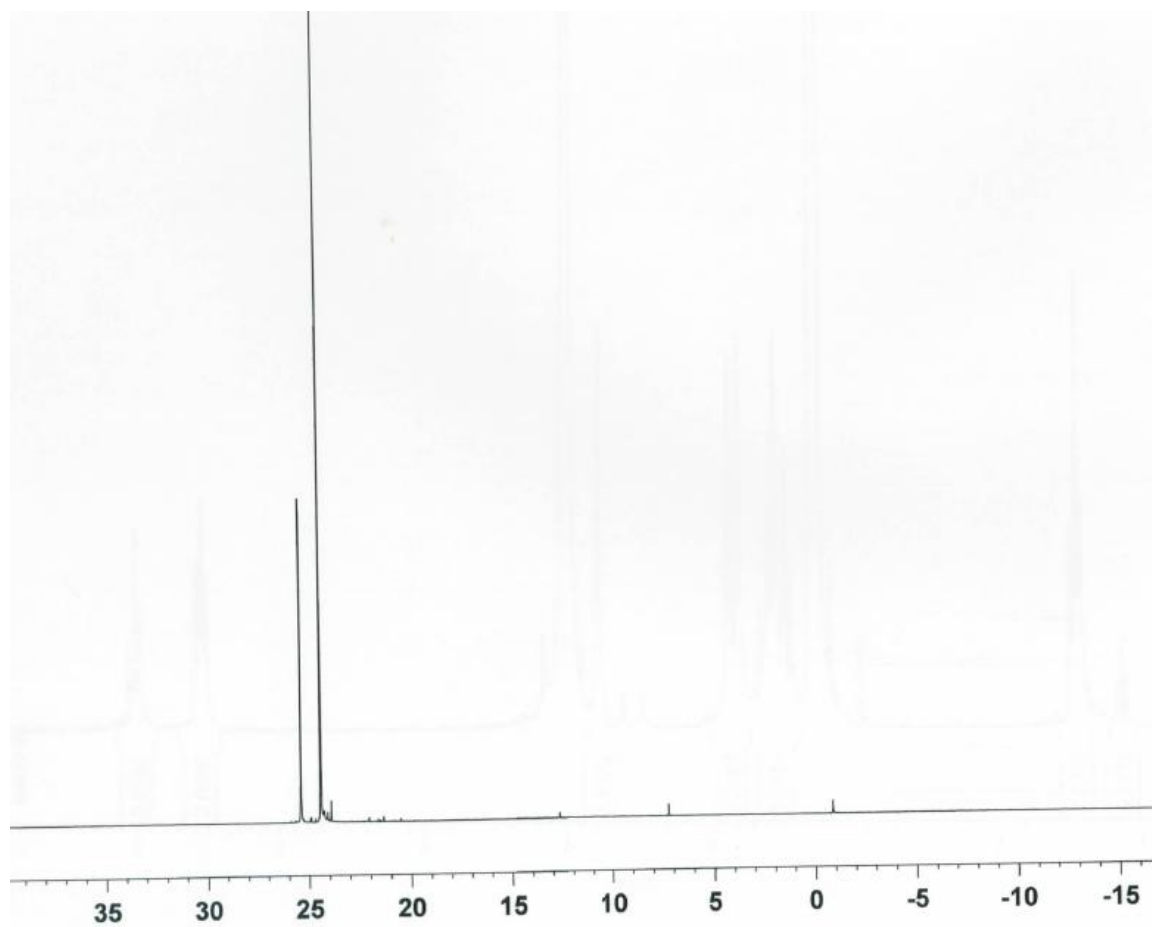


Figure S32. ^{31}P -NMR spectrum of compound **9** (CDCl_3 , 161.9 MHz).

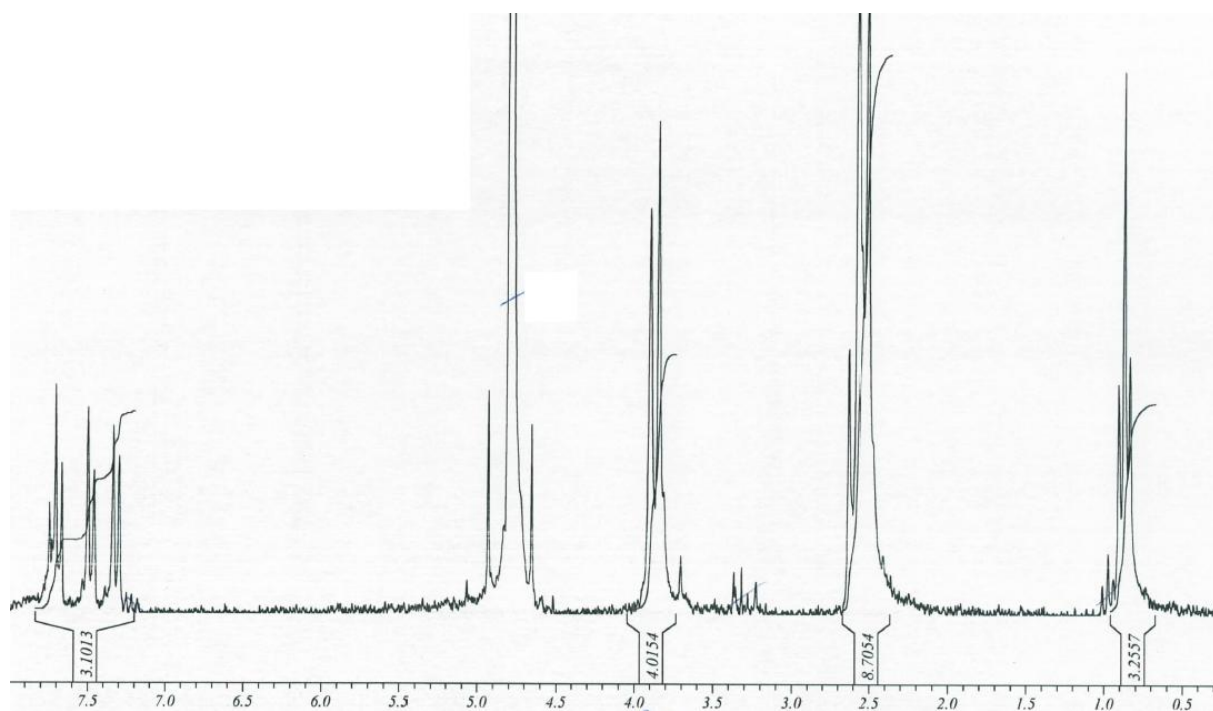


Figure S33. ^1H -NMR spectrum of Ligand L^3 ($\text{D}_2\text{O} + \text{NaOD}$, 200 MHz).

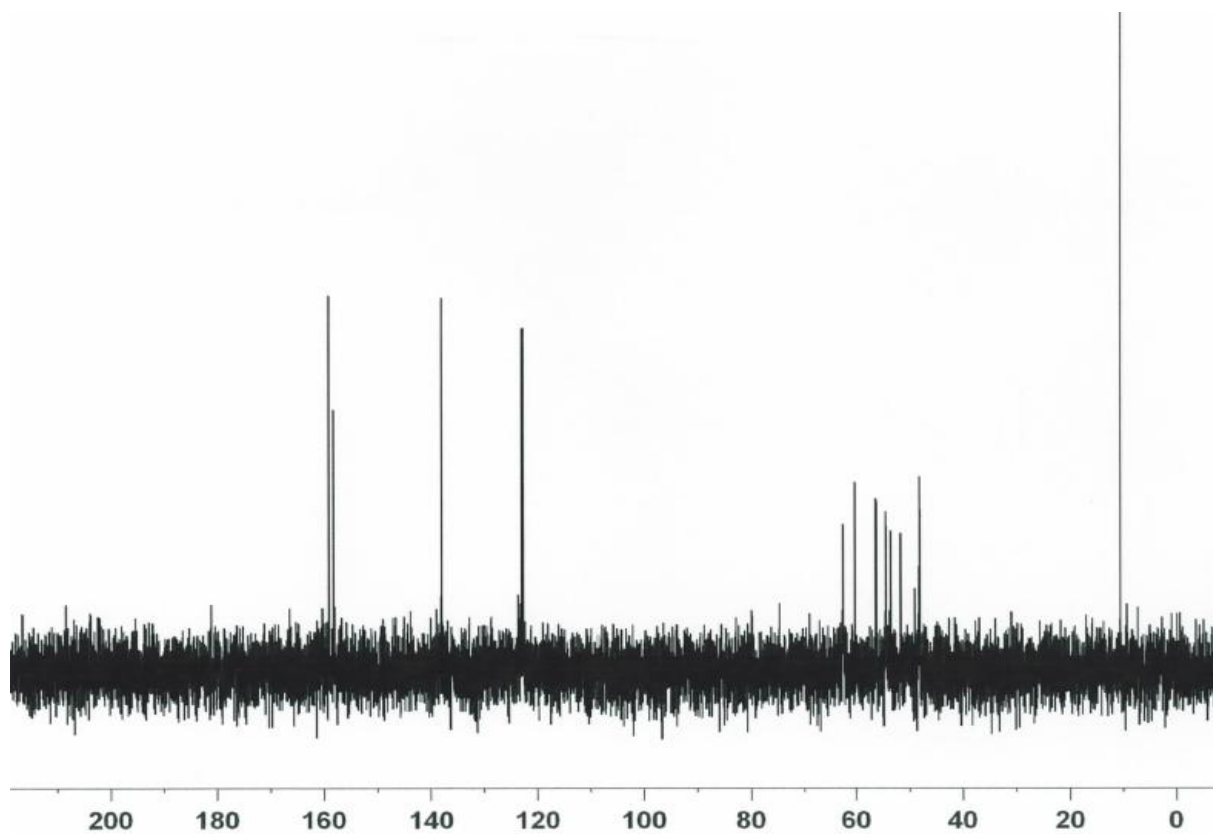


Figure S34. ^{13}C -NMR spectrum of Ligand L^3 (D_2O , 75 MHz).

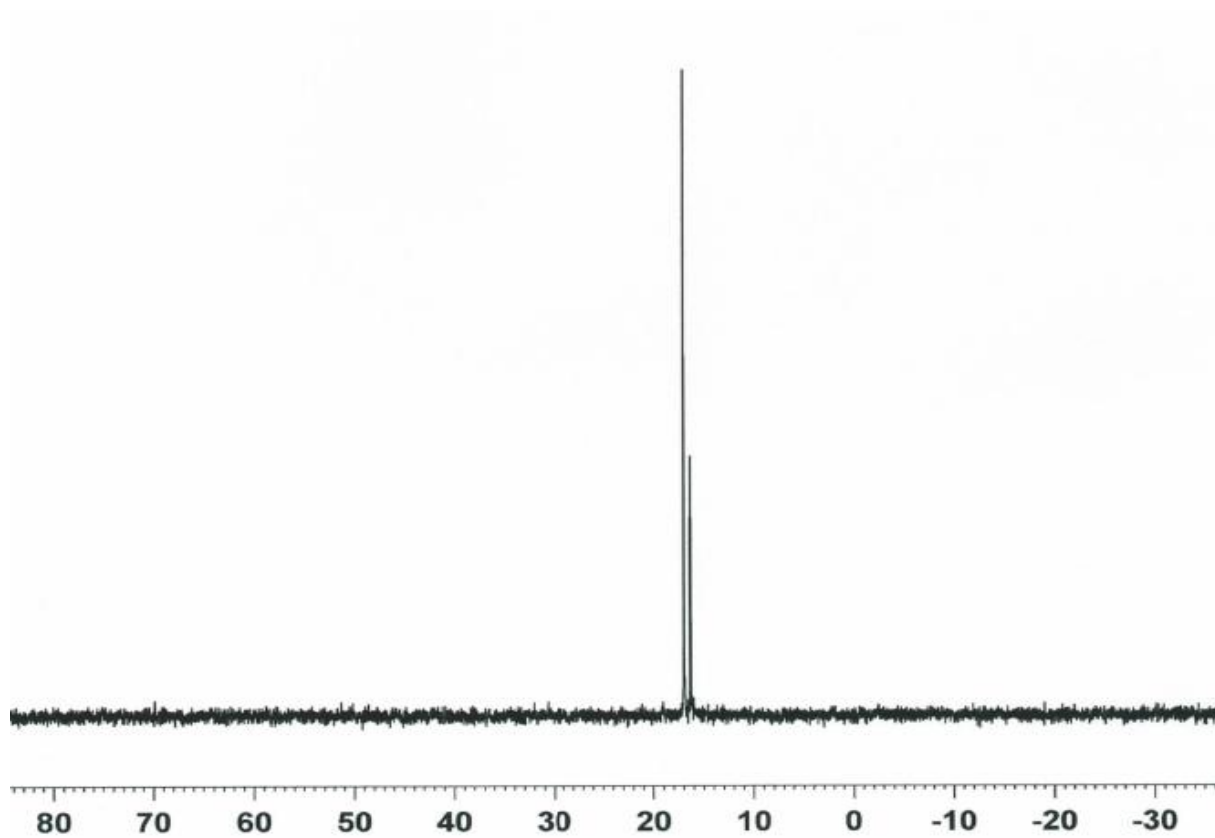


Figure S35. ^{31}P -NMR spectrum of Ligand **L**³ (D_2O , 161.9 MHz).

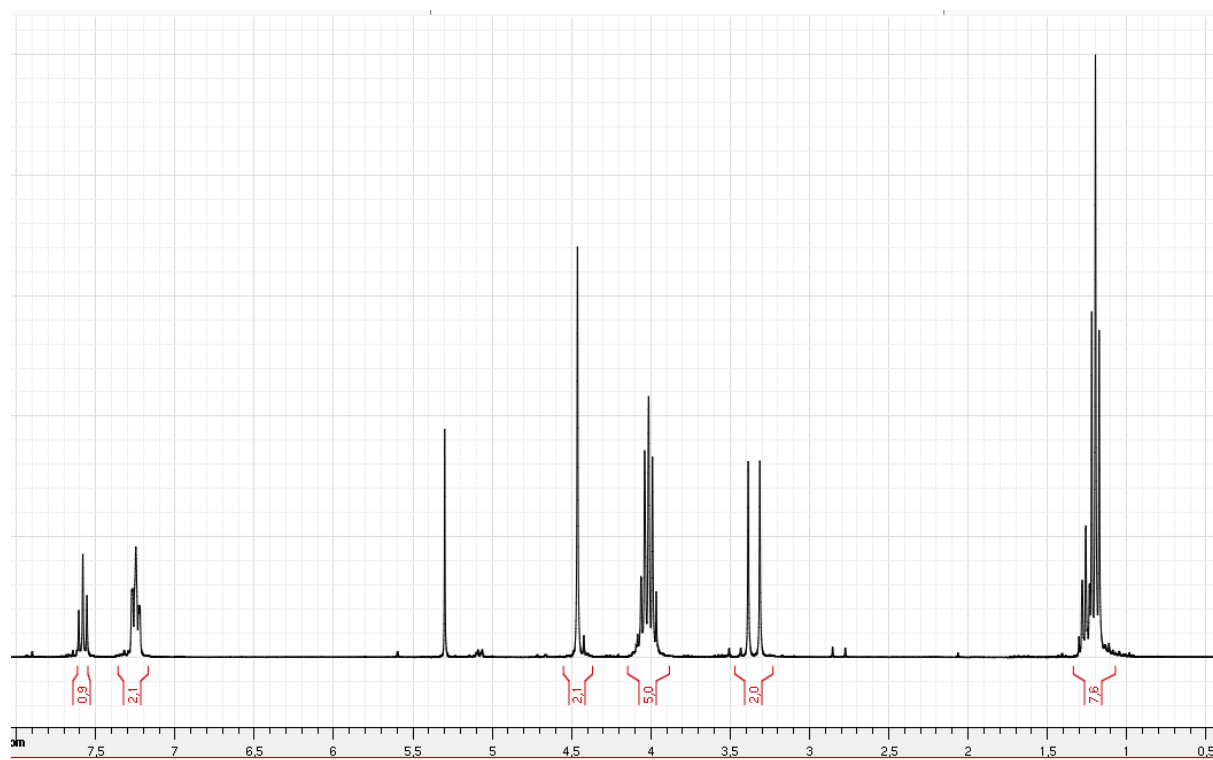


Figure S36. ^1H -NMR spectrum of compound **10** (CDCl_3 , 300 MHz).

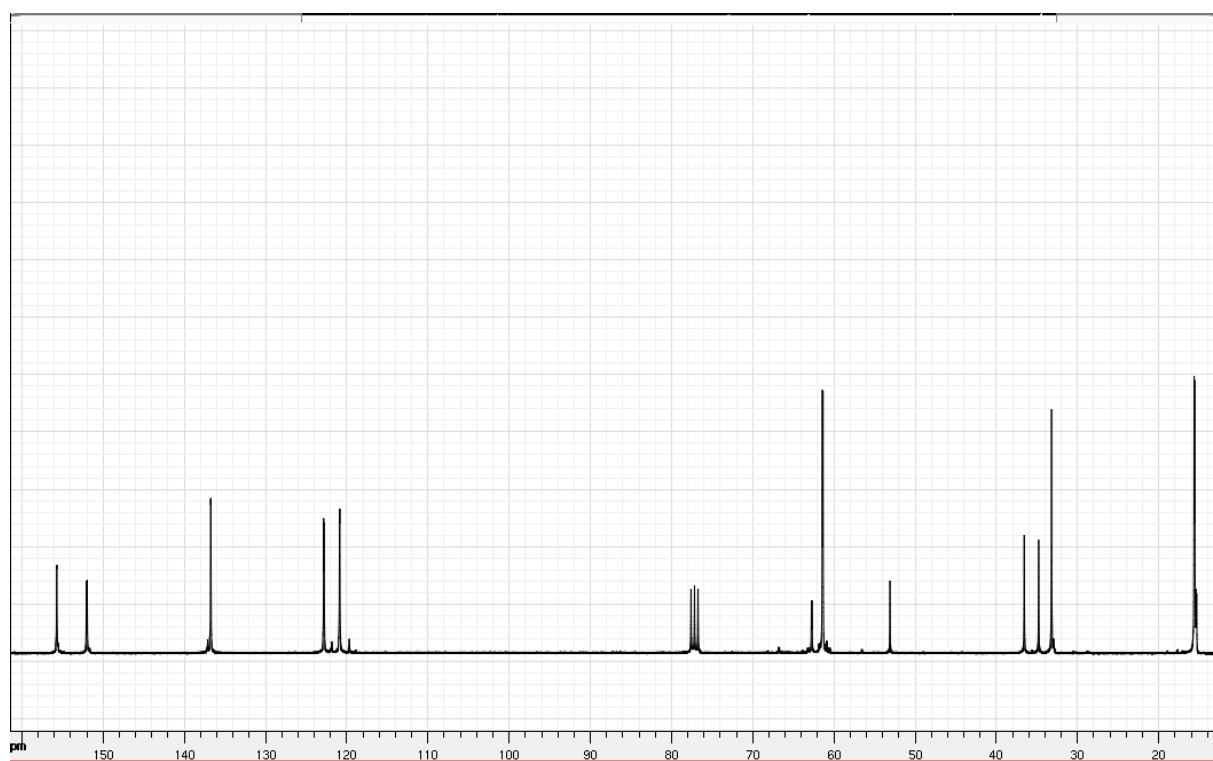


Figure S37. ^{13}C -NMR spectrum of compound **10** (CDCl_3 , 75 MHz).

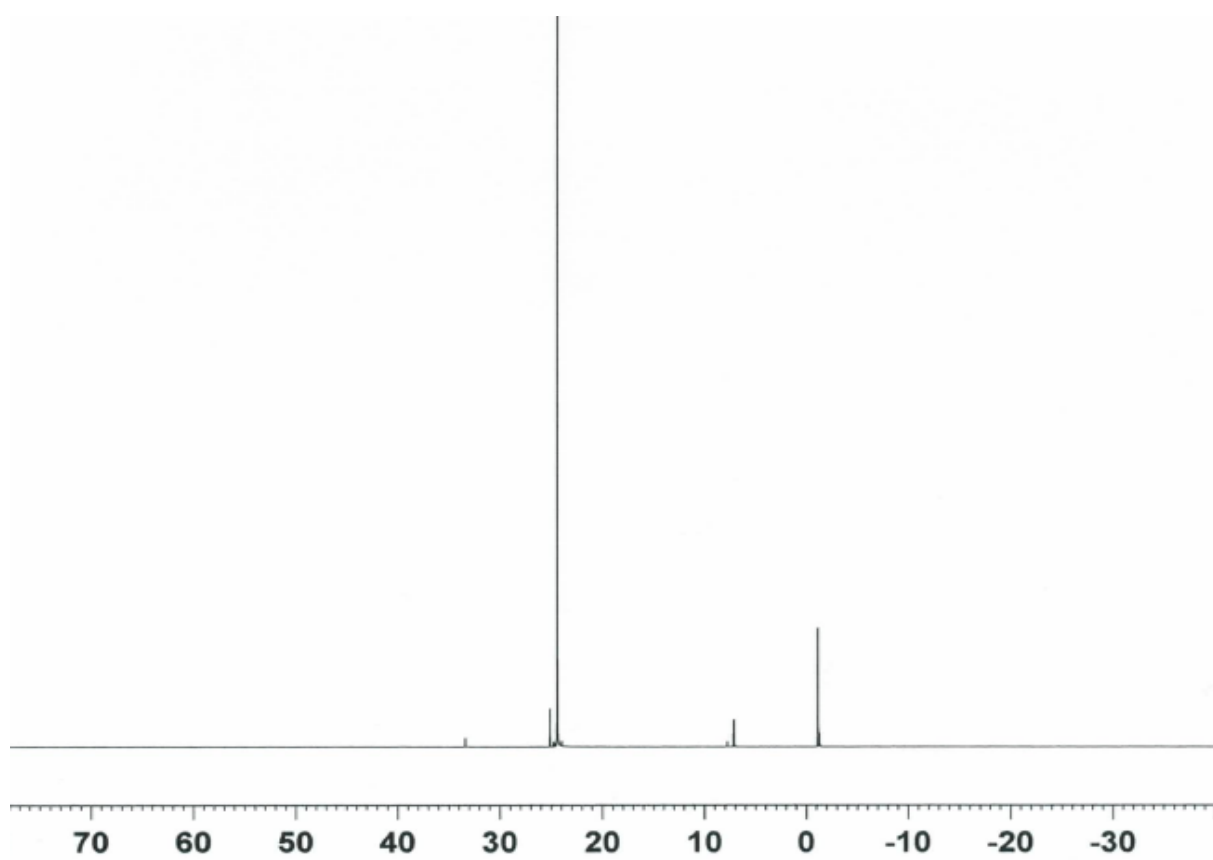


Figure S38. ^{31}P -NMR spectrum of compound **10** (CDCl_3 , 161.9 MHz).

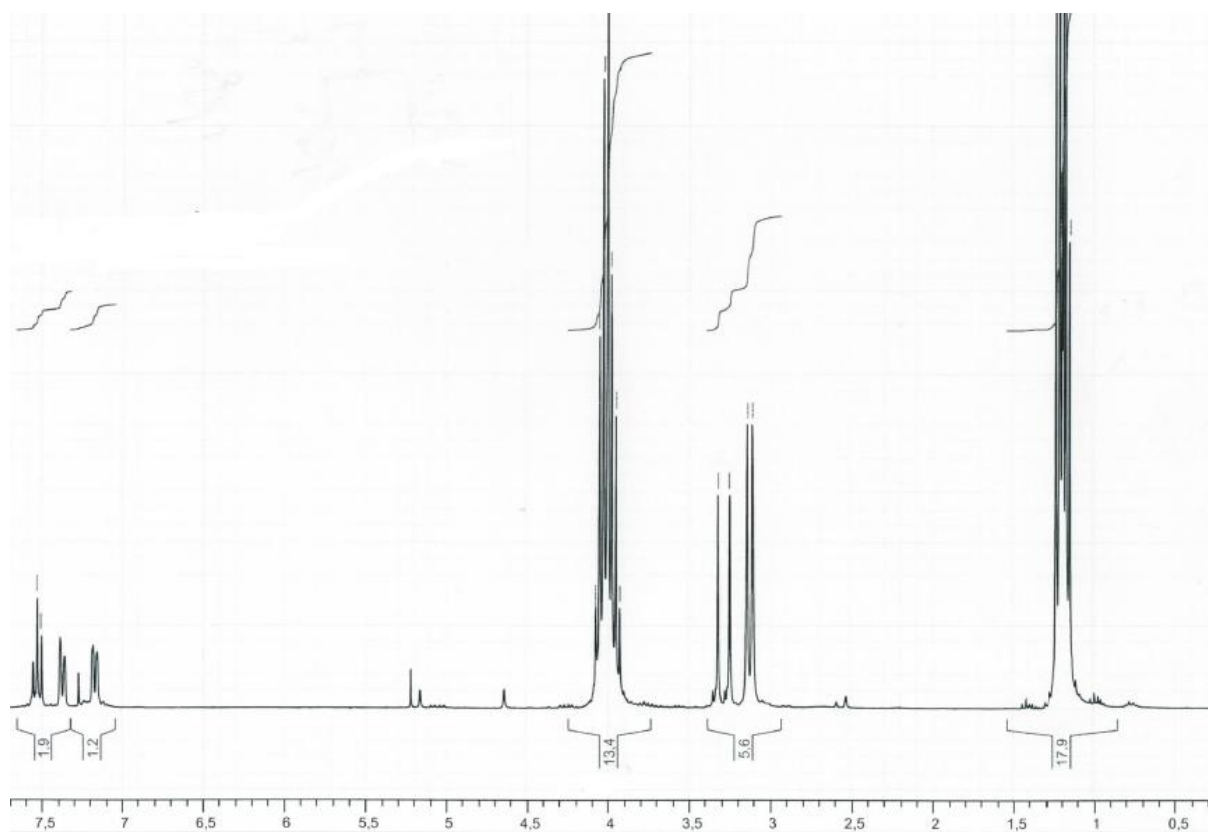


Figure S39. ^1H -NMR spectrum of compound **11** (CDCl_3 , 300 MHz).

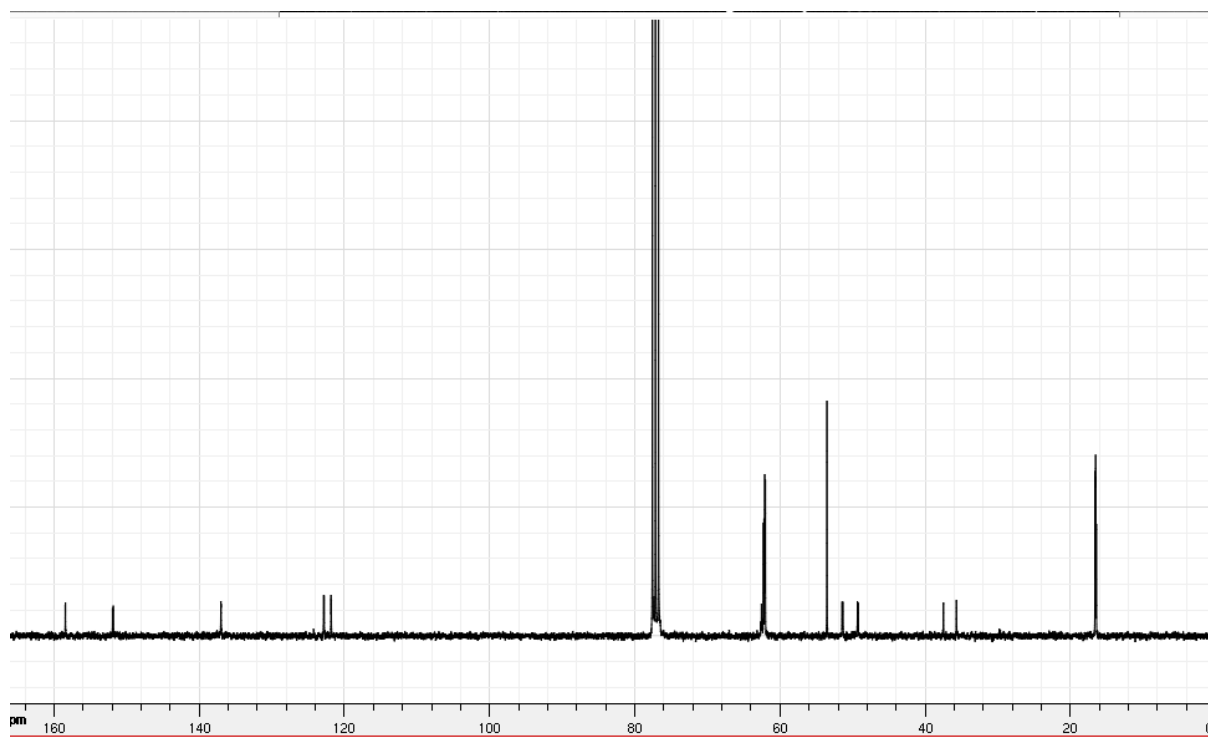


Figure S40. ^{13}C -NMR spectrum of compound **11** (CDCl_3 , 75 MHz).

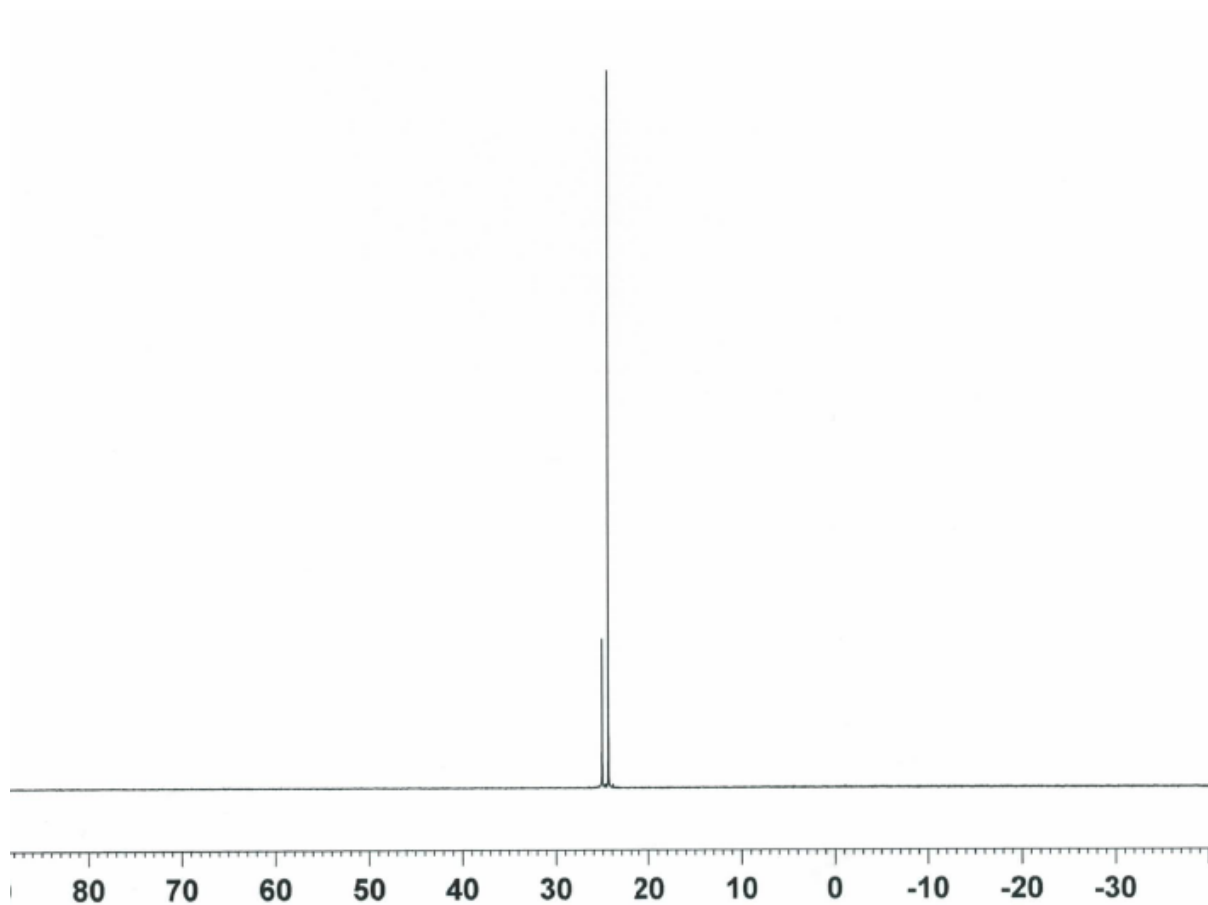


Figure S41. ^{31}P -NMR spectrum of compound **11** (CDCl_3 , 161.9 MHz).

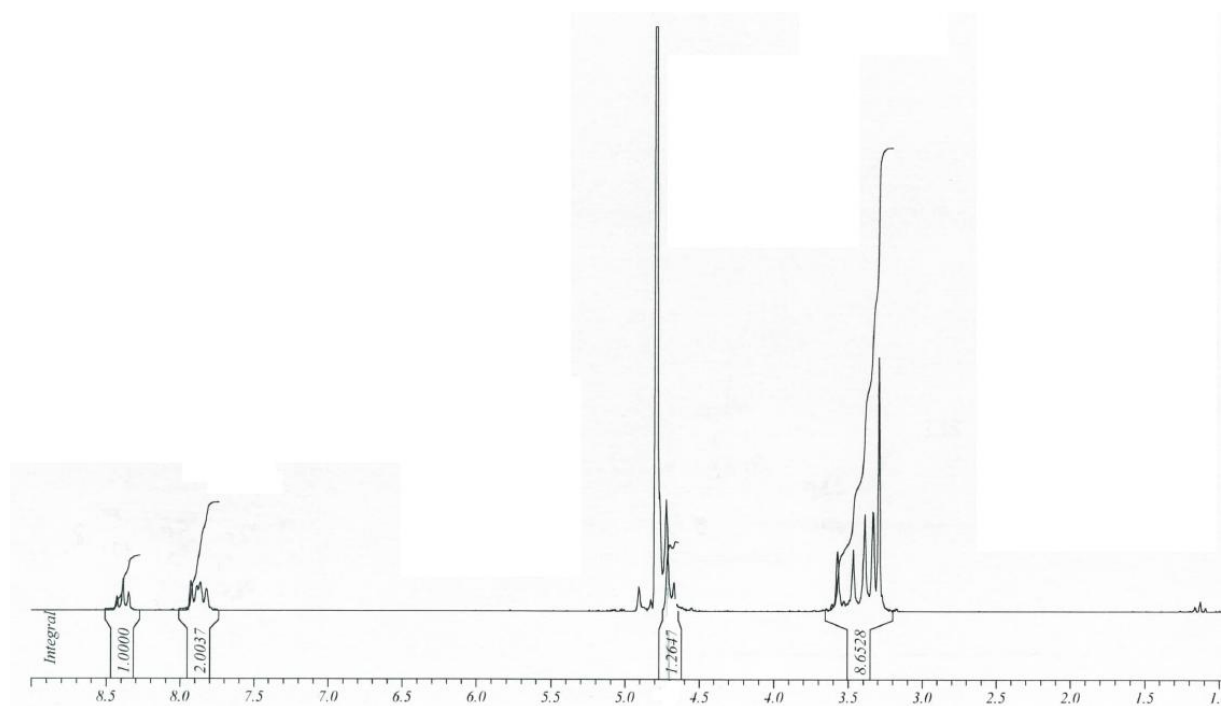


Figure S42. ^1H -NMR spectrum of Ligand **L⁴** (D_2O , 200 MHz).

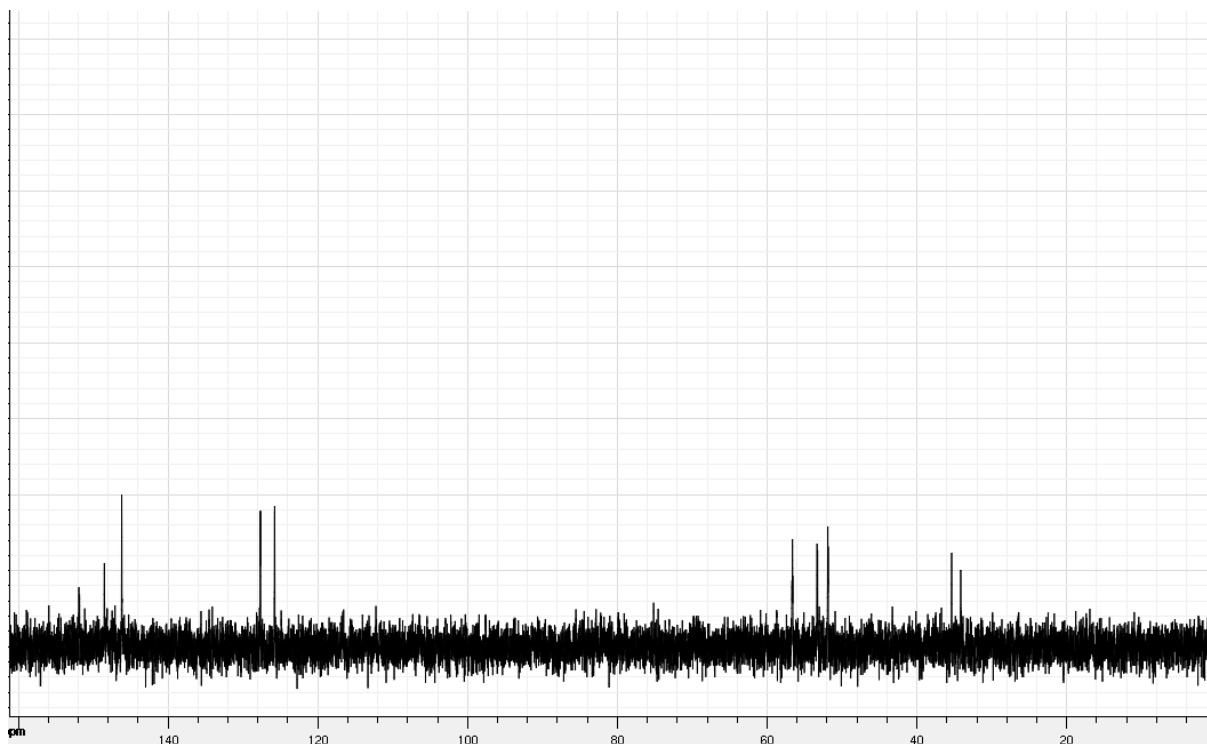


Figure S43. ^{13}C -NMR spectrum of Ligand L^4 (D_2O , 100 MHz).

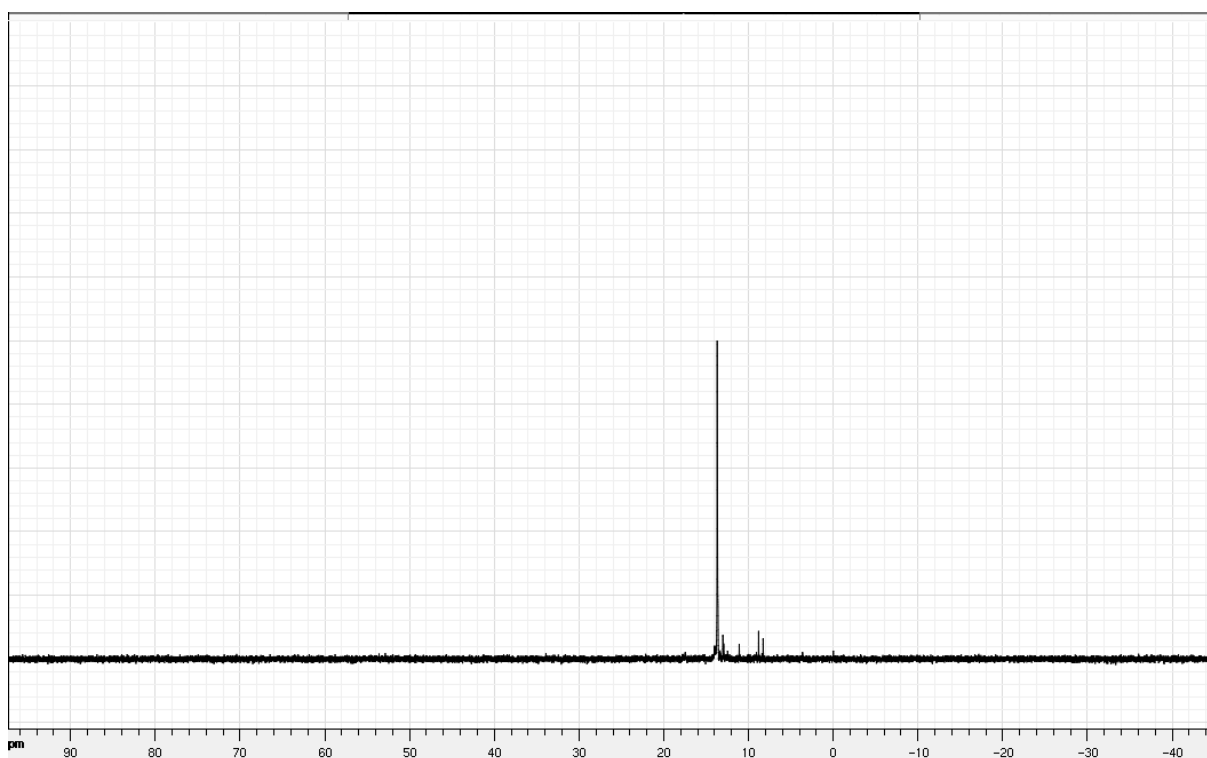


Figure S44. ^{31}P -NMR spectrum of Ligand L^4 (D_2O , 161.9 MHz).

Table S1. Stability and protonation constants of the metallic complexes with Ni(II), Zn(II), and Co(II) formed with ligands **L**¹-**L**⁴.

Equilibrium	$\log K_{\text{CuLH}_x}(3\sigma)$			
	L ¹	L ²	L ³	L ⁴
$\text{L} + \text{Ni} \xrightleftharpoons{K_{\text{NiL}}} \text{NiL}$	16.50(3)	14.34(6)	18.2(2)	18.1(4)
$\text{NiL} + \text{H} \xrightleftharpoons{K_{\text{NiLH}}} \text{NiLH}$	8.90(4)	6.89(6)	8.0(3)	6.9(4)
$\text{NiLH} + \text{H} \xrightleftharpoons{K_{\text{NiLH}_2}} \text{NiLH}_2$	7.55(5)	5.47(7)	5.9(3)	5.3(5)
$\text{NiLH}_2 + \text{H} \xrightleftharpoons{K_{\text{NiLH}_3}} \text{NiLH}_3$	5.85(5)	-	4.6(3)	
$\text{NiLH}_3 + \text{H} \xrightleftharpoons{K_{\text{NiLH}_4}} \text{NiLH}_4$	4.80(5)	-		
Equilibrium	$\log K_{\text{CuLH}_x}(3\sigma)$			
	L ¹	L ²	L ³	L ⁴
$\text{L} + \text{Zn} \xrightleftharpoons{K_{\text{ZnL}}} \text{ZnL}$	17.84(4)	11.99(6)	17.2(2)	12.1(3)
$\text{ZnL} + \text{H} \xrightleftharpoons{K_{\text{ZnLH}}} \text{ZnLH}$	8.53(4)	9.54(7)	8.1(3)	8.5(4)
$\text{ZnLH} + \text{H} \xrightleftharpoons{K_{\text{ZnLH}_2}} \text{ZnLH}_2$	7.33(4)	4.70(7)	4.6(3)	5.9(4)
$\text{ZnLH}_2 + \text{H} \xrightleftharpoons{K_{\text{ZnLH}_3}} \text{ZnLH}_3$	4.84(4)		4.6(3)	
$\text{ZnLH}_3 + \text{H} \xrightleftharpoons{K_{\text{ZnLH}_4}} \text{ZnLH}_4$	4.31(5)			
Equilibrium	$\log K_{\text{CuLH}_x}(3\sigma)$			
	L ¹	L ²	L ³	L ⁴
$\text{L} + \text{Co} \xrightleftharpoons{K_{\text{CoL}}} \text{CoL}$	16.50(9)	13.9(1)		
$\text{CoL} + \text{H} \xrightleftharpoons{K_{\text{CoLH}}} \text{CoLH}$	8.8(1)	6.4(1)		
$\text{CoLH} + \text{H} \xrightleftharpoons{K_{\text{CoLH}_2}} \text{CoLH}_2$	6.9(1)	4.5(2)		
$\text{CoLH}_2 + \text{H} \xrightleftharpoons{K_{\text{CoLH}_3}} \text{CoLH}_3$	5.4(1)			
$\text{CoLH}_3 + \text{H} \xrightleftharpoons{K_{\text{CoLH}_4}} \text{CoLH}_4$	4.8(1)			
Solvent: H ₂ O; <i>I</i> = 0.1 M; <i>T</i> = 25.0(2) °C. Error = 3σ with σ = standard deviation. $K_{\text{MLH}_x} = [\text{MLH}_x]/[[\text{MLH}_{(x-1)}][\text{H}]$ with M = Ni(II), Zn(II), Co(II) or Ga(III). Charges have been omitted for the sake of clarity.				

Table S2. Intensity maxima of the ESI-MS pseudo-molecular ions of the metallic complexes formed with ligands L^1 - L^4 .

L^1		L^2	
Pseudo-molecular ions	m/z exp. (calc.)	Pseudo-molecular ions	m/z exp. (calc.)
$[L^1H_8 + H]^+$	514.15 (514.03)	$[L^2H_4 + H]^+$	382.20 (382.13)
$[CuL^1H_6 + H]^+$	575.09 (574.95)	$[CuL^2H_2 + H]^+$	443.15 (443.05)
$[CuL^1H_6 + Na]^+$	597.10 (596.93)	$[CuL^2H_2 + Na]^+$	465.15 (465.06)
$[NiL^1H_6 + H]^+$	570.09 (569.96)	$[NiL^2H_2 + H]^+$	438.15 (438.05)
$[ZnL^1H_6 + H]^+$	575.68 (575.94)	$[ZnL^2H_2 + H]^+$	444.15 (444.04)
$[ZnL^1H_6 + Na]^+$	597.78 (597.92)	$[ZnL^2H_2 + Na]^+$	466.15 (466.03)
$[ZnL^1H_5 + 2Na]^+$	619.89 (619.90)		
L^3		L^4	
Pseudo-molecular ions	m/z exp. (calc.)	Pseudo-molecular ions	m/z exp. (calc.)
$[L^3H_6 + H]^+$	448.20 (448.08)	$[L^4H_6 + H]^+$	391.10 (391.02)
$[CuL^3H_4 + H]^+$	509.1 (509.00)	$[CuL^4H_4 + H]^+$	452.05 (451.95)
$[CuL^3H_4 + Na]^+$	531.10 (530.99)	$[CuL^4H_4 + Na]^+$	474.00 (473.93)
$[NiL^3H_4 + H]^+$	504.15 (504.00)	$[NiL^4H_4 + H]^+$	447.05 (446.94)
$[ZnL^3H_4 + H]^+$	510.15 (509.99)	$[ZnL^4H_4 + H]^+$	453.05 (452.94)
Solvent: H ₂ O. Positive mode; skimmer voltage ranges from 140 V to 170 V. In the case of Zn(II) complexes, a volatile ammonium acetate buffer has been employed. $[L]_{tot} \sim 3-4 \times 10^{-4}$ M. $[M(II)]_{tot}/[L]_{tot} \sim 1$.			